N. Jb. Geol. Paläont. Abh. 292/2 (2019), 129–154
Stuttgart, May 2019

Article

Facies analysis, sedimentary environment and sequence stratigraphy of the Khan Formation in the Kalmard Sub-Block, Central Iran: implications for Lower Permian palaeogeography

Samira Taghdisi Nikbakht, Payman Rezaee, Reza Moussavi-Harami, Mohammad Khanehbad, and Farzin Ghaemi

With 11 figures

Abstract: The Lower Permian Khan Formation in the Kalmard Sub-Block consists mainly of alternation of siliciclastic (conglomerate, sandstone, siltstone and shale) and carbonate rocks (limestones and dolostones), which were deposited in diverse coastal and shallow marine environments. The siliciclastic successions reflect several nearshore lithofacies, which constitute five major palaeoenvironmental associations including proximal lower-middle shoreface, upper shoreface, foreshore, tidal inlet and washover fan/lagoon. The most abundant sedimentary structures in the Khan Formation sandstones are horizontal lamination, planar and trough cross stratification, bidirectional plane bed, swaley and hummocky cross stratification. These successions were formed in a barrier island complex. Carbonate production in this formation is dominated by benthic foraminifera particularly fusulinids, brachiopods, mollusks, bryozoans, echinoderms, corals, *Tubiphytes*, ooids, intraclasts, and peloids. Based on fossil content, texture and sedimentary structures, 23 different facies types have been distinguished that accumulated in four facies associations. The majority of facies associations (FA1–FA4) were formed in tidal flat (FA1), lagoon (FA2), bioclastic shoal (FA3) and shallow open marine (FA4) which deposited on a homoclinal ramp including inner and middle ramp. On the basis of facies relationships and the recognition of key surfaces in the Khan Formation, four (in the Bakhshi and Bibisene sections) and three depositional sequences (in the Tangal-e-Shotoru and Rahdar sections) are recognized. The stratigraphic architectures of the Khan Formation deposits are the result of the interplay between activity of the Kalmard Fault and relative sea-level changes. Palaeogeographic data show that during the deposition of the Khan Formation, the Kalmard Sub-Block was located in low latitudes in a warm and humid climate.

Key words: Homoclinal ramp, shoreface, Lower Permian, Khan Formation, Iran..

1. Introduction

The Khan Formation is a thick carbonate-siliciclastic sequence sporadically exposed in several places in the Kalmard area (Aghanabati 1977). Four stratigraphic sections (NE–SW transects) of the Khan Formation in the Kalmard Sub-Block were measured and sampled for this study (Figs. 1, 2) comprising the Bakhshi section (type section of Khan Formation), which is located in the southeast of Kalmard Karevansaray, approximately 92 km west of Tabas, the Tangal-e-Shotoru section, which is located 55 km west of Tabas, the Rahdar section about 50 km west of Tabas, and the Bibisene section, 80 km northwest of Tabas (Fig. 1). The thickness of the Khan Formation in the Bakhshi, Tangal-e-Shotoru, Rahdar and Bibisene sections is 295, 202, 199 and 427 m, respectively (Fig. 3). It consists mostly of cyclic sequences

DOI: 10.1127/njgpa/2019/0812
www.schweizerbart.de
0077-7749/2019/0812 $ 6.50

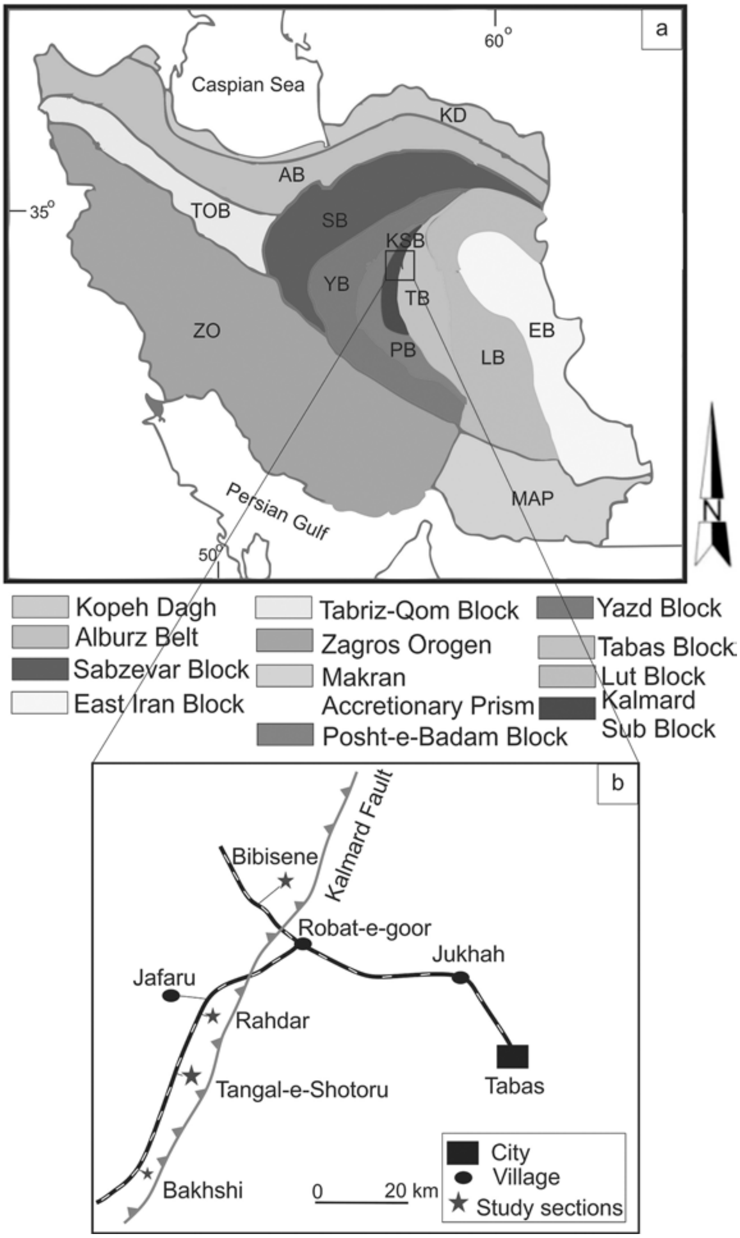

Fig. 1. (a) Generalized tectonic map of Iran (after Alavi 1991), (b) location map of the study sections of the Khan Formation.

starting with sandstones and ending with limestones and dolostones. The size of clasts in sandstones increases upward, and the topmost portion of each cycle is a light to dark gray, medium- to thick-bedded shallow water wackestone, packstone and grainstone intercalated with muddy limestone, dolomitic limestone and dolostone. Many sedimentary structures (physical and biogenetic sedimentary structures) are found in the Khan Formation. All these structures have considerable environmental and palaeocurrent importance which can be very useful for the basin analysis of this formation.

The aim of this study is to examine the depositional facies, sedimentary environments and sequence stratigraphy of the Lower Permian (Khan Formation) successions exposed in the Kalmard Sub-Block. The aforementioned well-exposed successions provide a favorable opportunity to study the vertical and lateral

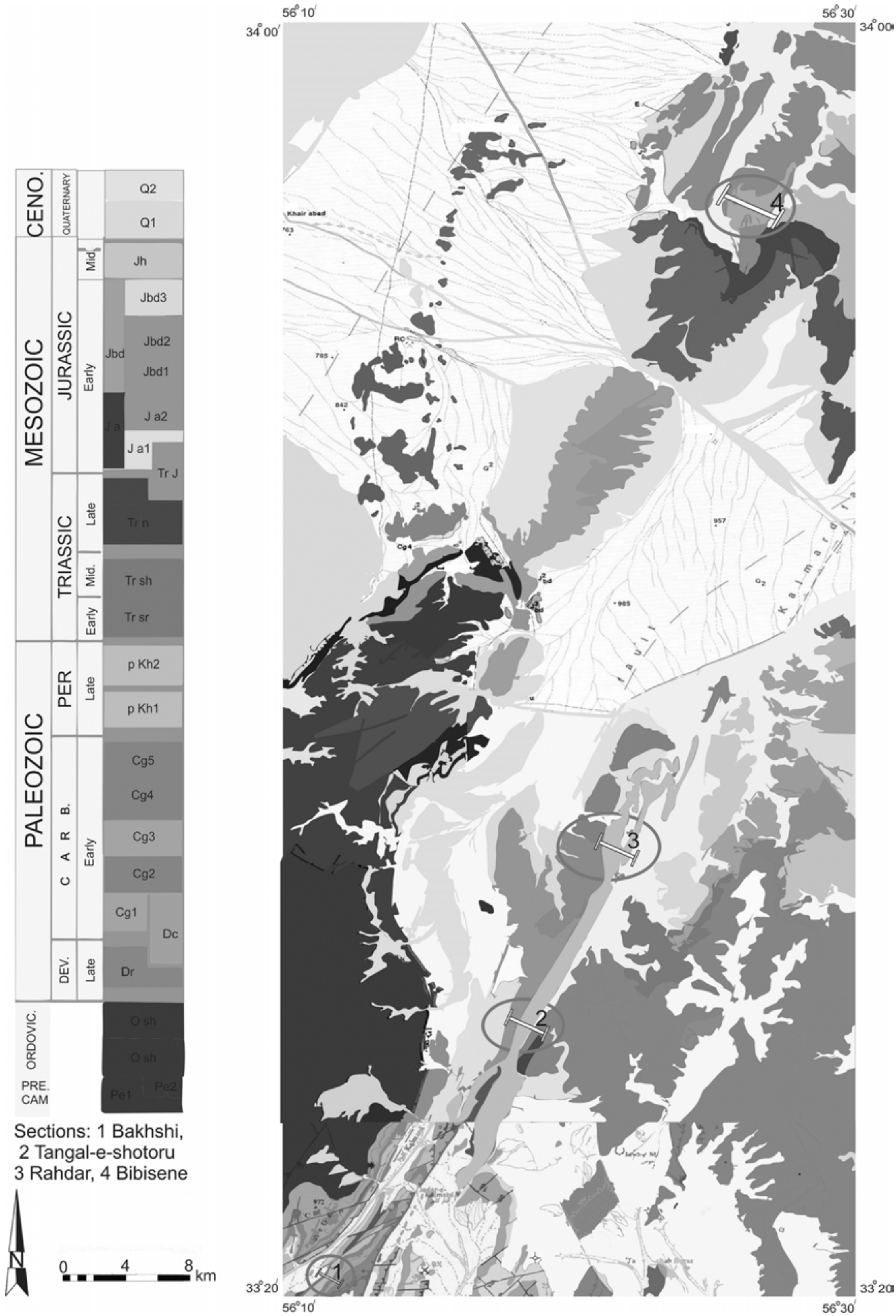

Fig. 2. Geological map of the Khan Formation in the Kalmard area (modified from AZHDARI 1999; SHIEKHOLSLAMI & ZAMANI 1999), with four study sections.

Fig. 3. The stratigraphic sections (Bakhshi, Tangal-e-Shotoru, Rahdar and Bibisene) of the Lower Permian Khan Formation showing the sedimentological characteristics, depositional environments and sequence stratigraphic units.

facies variations of different environments in detail via sequence stratigraphy that can help for the reconstruction of the Lower Permian palaeogeography in Central Iran.

2. Geological setting

Iran is divided into several tectonic provinces based on several structural and sedimentary features (Stocklin 1968; Stampfli 1978; Eftekharnezhad 1980; Berberian & King 1981; Alavi 1991). Central Iran is one of the most active provinces which has been divided into four tectonic blocks including the Lut, Tabas, Posht-e-Badam and Yazd blocks (Fig. 1) according to Alavi (1991). The Kalmard Sub-Block, in the west of Tabas town, is narrow and sandwiched between the Posht-e-Badam and Tabas blocks, and stretches along the large Kalmard Fault (Ernst & Gorgij 2013). The Kalmard Sub-Block studied in this paper is located between 31° 51′ 5″ N and 55° 59′ 30″ E and separated from the Tabas Block by the Kalmard and Kuhbanan faults. Aghanabati (2004) considered the Kalmard area as a part of the Tabas Block based on a strong resemblance of the Precambrian basement in the Kalmard and Tabas areas. Since the Kalmard area is located between two active faults (Kalmard Fault in the East and the covered Naeini Fault in the West), he proposed that it is possible to designate this area as an isolated sub-block within the Tabas Block.

The Permian strata (Khan Formation) in the Kalmard Sub-Block (Central Iran) were deposited in a shallow marine environment (Aghanabati 2004). Recent biostratigraphic studies on this formation, based on fusulinids and colonial corals, suggest a late Sakmarian to early Artinskian age (Davydov & Arefifard 2007; Badpa et al. 2014). Early Permian successions in the north of the Kalmard region are recognized by the formal Khan Group showing various features in different outcrops. This group is made up of three different informal formations from lower to upper parts: Chili, Sartakht and Hermez (Shahraki et al. 2015; Emraninasab et al. 2016; Emraninasab et al. 2017). The lower boundary of the Khan Formation is located above the disconformity of the Carboniferous Gachal Formation. It is overlain by the Lower Triassic yellow vermiculite limestone of the Sorkh Shale Formation with a disconformity marked by a bauxite horizon (Figs. 2, 3).

3. Material and methods

Four complete stratigraphic sections were selected at the well-developed Lower Permian successions of the Khan Formation (Fig. 1). The studied sections were measured, sampled and described bed-by-bed for lithological changes and sedimentary structures. 500 rock samples were collected and examined in 481 thin sections for the determination of the lithofacies. The sandstone lithofacies were described following the classification of Pettijohn et al. (1987). The terminology for the environmental zonation of siliciclastic successions was based on MacEachern & Pemberton (1992), MacEachern et al. (1999a) and MacEachern et al. (1999b) who separated the shoreface and offshore environments from those of the shelf. Limestone microfacies were described following the classification of Dunham (1962), with the modifications of Embry & Klovan (1972). Facies definition was based on the microfacies characteristics, including depositional texture, grain size, grain composition, and fossil content (Wilson 1975; Flügel 2010). Recognition of depositional sequences and sea-level changes were interpreted based on the studies of Catuneanu (Catuneanu et al. 2009; Catuneanu et al. 2011; Catuneanu et al. 2013).

4. Siliciclastic facies

The siliciclastic sediments are widely distributed and present in all studied sections. The grains mostly consist of monocrystalline quartz, chert, lithic sandstone and reworked carbonate grains such as eroded skeletal grains. The lithofacies group is composed of a variety of gravel, sand and silt- to clay-sized grains. Conglomerate usually occurs at the base of the successions and exhibits massive structures. Sandstone has sedimentary structures such as horizontal lamination, planar and trough cross lamination, swaley and hummocky cross stratification and normal and reverse graded bedding. Siliciclastic mudstones are seen between the sandstone beds. Quartz arenites are the dominant lithofacies in the siliciclastic deposits of the Khan Formation which have a good textural and mineralogical maturity. Based on the sedimentological and stratigraphic framework, the siliciclastic facies of the Khan Formation are differentiated into the following facies.

4.1. Facies A: Proximal lower-middle shoreface

This facies is dominated by thin to thick (10–40 cm), laterally extensive, sharp erosional basal contact, and fine- to medium-grained sandstones which is made of thoroughly amalgamated, well-to medium-sorted sandstone units. The dominant sedimentary structures

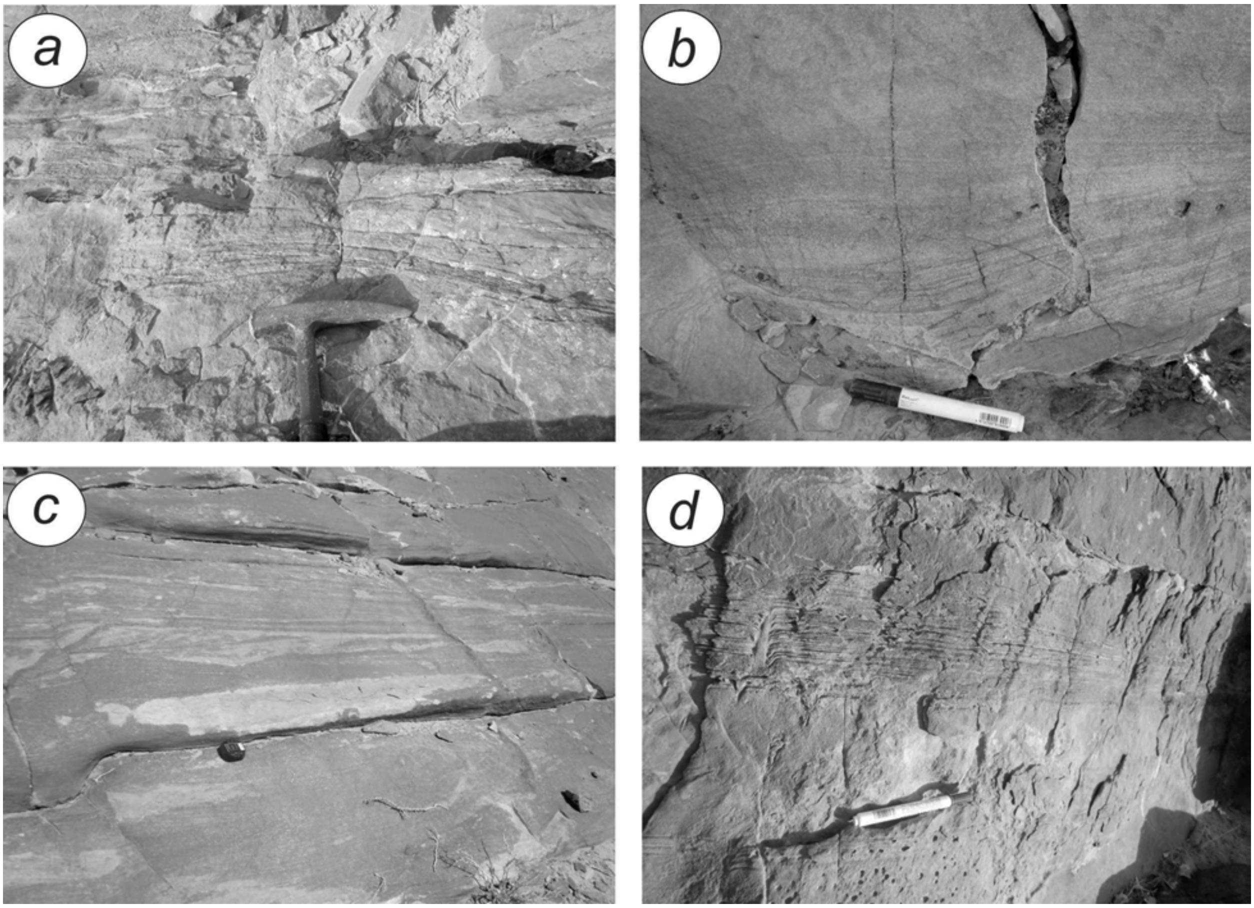

Fig. 4. Sedimentary structures of proximal lower-middle shoreface facies (a, b) Thin beds and laminations of sandstone of proximal lower-middle shoreface (Facies A) contain HCS, planar lamination and bedding. (c) Thickly amalgamated tabular cross-stratified and hummocky beds in fine- to medium-grained sandstone in the middle shoreface facies. (d) Massive and planar lamination as well as the bedding of fine- to medium-grained sandstone with *fugichnia* in the middle shoreface facies.

consist of massive sandstone as well as low-angle, parallel- and hummocky/swaley cross-stratified sandstones (Figs. 3, 4a–d). Some of parallel laminated sandstone is considered to represent the internal expression of SCS (Leckie & Walker 1982). Palaeocurrent data from tabular cross-bedding sets give northeast/south-west palaeoflow directions orientated approximately parallel to the inferred depositional strike. *Fugichnia* (scape structures) can be observed in laminated fine-grained sandstone.

Interpretation: The sharp-based sandstone beds reflect deposition in a shallow marine environment below the fair-weather wave base. Massive sandstone may indicate deposition which has taken place in a proximal lower shoreface (e.g., Cheel & Leckie 1993; Myrow & Southard 1996; Myrow et al. 2002; Bayet-Goll et al. 2015a). The sedimentary structures in this facies reflect deposition in a high energy, storm-dominated environment influenced by a longshore current that formed thick, amalgamated tabular cross-beds. The transitions from proximal lower to middle shoreface include the increase of bed thickness of tempestites and the average wavelength of HCS (e.g., Myrow et al. 2002; Myrow et al. 2004). The occurrence of *fugichnia* in a sandstone is an indicator of tempestites or storm deposits (Haji Karim 2006). Considering the above characteristics, Facies A is interpreted as the product of sedimentation in the proximal lower-middle shoreface of a storm-dominated shoreline, below the fair-weather wave base.

4.2. Facies B: Upper shoreface

This Facies comprises meter-thick, well-sorted, weakly bioturbated, medium- to coarse-grained sandstone characterized by the presence of 10–35 cm thick sets of multidirectional trough cross-stratification and tabular cross-stratification sets. Cross-strata palaeocurrents are mainly oriented towards the northwest approximately perpendicular to the depositional strike; moreover, most units have little or no bioturbation (Fig. 5a, b).

Interpretation: The coarse grain size and the presence of abundant large-scale, trough to tabular cross-stratification indicate that much of this facies was deposited in a storm-dominated marine environment above the fair-weather wave base (Bayet-Goll et al. 2015b; Fa et al. 2015). High-angle cross-stratification is indicative of upper shoreface conditions in classical siliciclastic offshore-shoreface upward-shallowing successions (Hampson & Storms 2003). Additionally, it is typical of onshore migration of sandbars by nearshore currents in the surf zone during fair-weather periods (MacEachern et al. 2007; MacEachern & Bann 2008). Palaeocurrent data taken from trough cross-stratification indicates migration of large three-dimensional dunes within an upper shoreface environment. We interpreted this facies association, which have been formed by low-regime tractive processes generated by waves in the wave breaking and surf zones in an upper shoreface environment.

4.3. Facies C: Foreshore

This facies is composed of meter-thick, erosional-based, laterally continuous, sub-horizontal sets of clean and generally well-sorted, highly mature, and white to light gray sandstone that is predominantly coarse- to very coarse- grained with basal micro-conglomerate (Fig. 5c, d). Amalgamated beds of this facies are up to 3 m thick and horizontal to low-angle laminations (oriented parallel to depositional strike) that are the most common sedimentary structures with occasional small scale cross-laminations (Fig. 5d). The low-angle laminations mainly dip (1–3°) in an offshore (NW) direction that corresponds to the beach face. This facies is not intensely bioturbated, and the trace fossil diversity is generally very low. Besides, there are only some plant fossils in some areas coated by iron oxide (upper parts of the Rahdar and Tangal-e-Shotoru sections) (Fig. 5e).

Interpretation: The well-developed horizontal lamination, a high degree of sorting, and the lateral continuity of sandstone beds are all the evidence for a foreshore deposit. The parallel lamination reflects high energy swash and backwash transport which is typical of beach deposits. The foreshore facies association occurs at the top of the barrier between 1 m below and 2 m above the palaeo-sea-level (e.g., Seidler & Steel 2001). Trough cross-stratification resulted from dune migration under wave-generated onshore-directed sediment transport. Little or no bioturbation in these deposits can be attributed to the abundance of well-winnowed sand, the general paucity of food particles for deposit feeders, the probable high energy currents as well as high sedimentation rates in foreshore settings (e.g., Pemberton & MacEachern 1997; Buatois & Mangano 2011).

4.4. Facies D: Tidal inlet

This facies consists of laterally discontinuous, lens-like units of medium-bedded (~20–35 cm), medium- to coarse-grained, medium- to poorly-sorted sandstone. The facies is dominated by thick tabular and trough cross-bed sets. In some areas, the angle of repose of cross-bed sets shows oppositely dipping foresets in superimposed beds which result in a bidirectional pattern. Superimposed beds show basal and internal erosion surfaces with gravel lags on basal surfaces locally (Fig. 5f). This facies is generally in erosional contact with underlying deposits of Facies A, B and C; furthermore, most units have little or no bioturbation.

Interpretation: The extensive tabular cross-bedding reflects the transport of coarse-grained dunes in a deep channel. In addition, moderate to poor sediment sorting, bidirectional palaeocurrents (in bidirectional plane beds) together with the lenticular geometry and the erosional base also support the interpretation of this facies as a tidal inlet. The lack of trace fossils suggests a paucity of organisms probably due to high energy currents and high sedimentation rates in tidal inlet settings.

4.5. Facies E: Washover fan/lagoon

Facies E is composed of interbedded fine-grained, well-sorted, medium-bedded (15–25 cm thick) red to brown sandstone (<45 %) and siliciclastic mudstone (siltstone and shale). The sandstone beds (Fig. 5g) are recognized by massive to horizontal-laminated sandstone locally with chert-pebbles, normal grading and basal erosional contact. Bauxite/laterite hori-

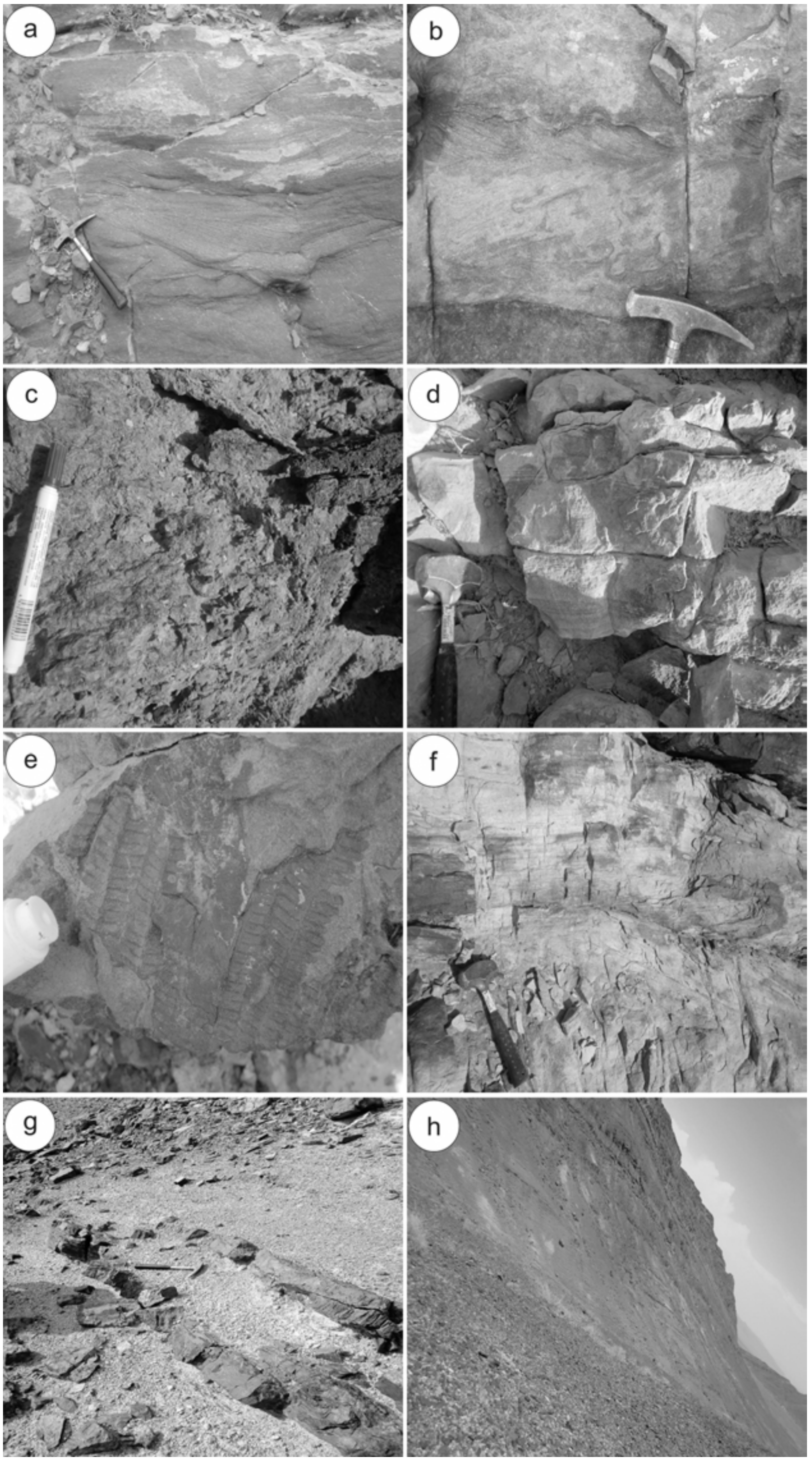

Fig. 5. Sedimentary structures of siliciclastic successions of the Khan Formation: (a, b) Outcrop photographs of the Facies C (Upper shoreface), trough cross-stratified sandstone (a) and decimeter-scale sets of tabular cross-stratification (b), (c) Conglomerate of foreshore facies contains chert pebbles at the base of the middle member of the Rahdar Formation, (d) Outcrop photographs of facies C (Foreshore), amalgamated sub-horizontal sets of well-sorted coarse-grained sandstone, (e) Plant fossils in foreshore sandstone in the uppermost part of the Rahdar section, (f) Bidirectional plane beds in tidal inlet sandstone (facies D) with an erosional base in the middle part of the Rahdar section, (g) Interlaminated and interbedded shale, siltstone and fine-grained sandstone of washover fan/lagoon facies (Facies E), (h) Bauxite/laterite in the uppermost part of washover fan/lagoon deposits in the Bakhshi section as SB1.

zons are observed in the uppermost part of the above-mentioned facies (Fig. 5h).

Interpretation: In general, facies E reflects deposition in a lagoonal environment periodically flooded by storm events. This facies is interpreted as an interfingering of washover fan sandstone beds with fine-grained lagoonal deposits behind a barrier island. The turbid water and fluctuating salinity from inflows may have made a poor habitat for most organisms. Therefore, bioturbation is much less intense here than in the shoreface facies. The sandstone beds have notable features which indicate single-event deposition such as normal grading. The low-diversity trace fossil assemblage in this facies is diagnostic for deposition in environments related to periodic salinity changes and oxygenation stresses as common in lagoonal settings (Pemberton et al. 1992a).

5. Carbonate facies

The carbonates of the Khan Formation are dominated by poorly to well-sorted skeletal and non-skeletal packstones to grainstones. Wackestones, mudstones and dolostones are the subordinate facies. Four facies associations (including 23 facies) are described on the basis of sedimentological features, composition, matrix grain size and fossil content that were deposited in a homoclinal ramp. The described facies associations are as follow:

5.1. Tidal flat facies association (FA1) (inner ramp)

The FA1 comprises of thin/medium-bedded mudstones/wackestones. In this facies association, detrital silt-size quartz grains and skeletal grains are present in low abundance. Facies association FA1 is divided into five facies according to the frequency, the type of carbonate grains and the matrix between the carbonate grains. These facies are described as below:

MF1: Lime mudstone: This facies consists of light gray, thin-bedded, mostly non-laminated and homogeneous lime mudstones. Scattered detrital silt-size quartz grains, scattered skeletal grains (bivalves) and fenestral fabric in some samples are also present (Fig. 6a). This microfacies is recognized in all sections of the Khan Formation. The main diagenetic feature in this facies includes the replacement of micrite by microspar (Fig. 6a).

MF2: Sandy lime mudstone: This facies is represented by light gray, thin-bedded, mostly non-laminated and homogeneous sandy lime mudstones. Lime mudstones contain only scattered skeletal grains (bivalves) and medium- to fine-grained, moderate to well-sorted, sub-rounded to rounded mono-crystalline quartz grains (about 10 % to 15 %)(Fig. 6b).

MF3: Dolomudstone: This facies consists of light gray, thin- to medium-bedded, dense, very-fine- to fine-grained dolomudstones (Fig. 6c). The size of the dolomite rhombs ranges from 5 to 16 µm (with a mean of 11 µm). The main features of this facies are subtly preserved depositional textures such as scattered detrital quartz grains. In places, the dolomite diagenetically recrystallized to coarser crystals.

MF4: Sandy dolomudstone: Light gray, medium beds of sandy dolomudstone are characteristic for this facies in the field. Dolostone crystals are fully dense, i.e., with no porosity. Medium- to fine-grained, moderate- to well-sorted, sub-rounded to rounded monocrystalline quartz grains represent about 10 % to 15 % of the rock. No relic of the original fabric is present in this facies. Additionally, the size of the dolomite rhombs ranges between 5 and 16 µm (Fig. 6d).

MF5: Diagenetic dolostones: Three types of dolomite crystals were identified in the Khan Formation which are dolomicrites (very fine crystalline dolomites), dolomicrosparites (fine crystalline dolomites) and dolosparites (medium crystalline dolomites). These dolomicrosparites have the relics of allochems such as bivalves and echinoderms. But the original sedimentary textures in the dolosparites of the Khan Formation are not preserved (Figs. 6e–g). In the Bibisene section dolostones are very abundant and the size of dolomite crystals increase upward (from dolomicrite to dolosparite).

The dolomicrites are considered to have formed during very early diagenesis in supratidal environments (Adabi 2004; Arefifard & Isaacson 2011). Based on the texture, fine crystals and the presence of quartz grains scattered in the dolomicrites, these dolomites were formed under near-surface low temperature conditions (Sibley & Gregg 1987; Gregg & Shelton 1990). The dolomicrosparites are formed by

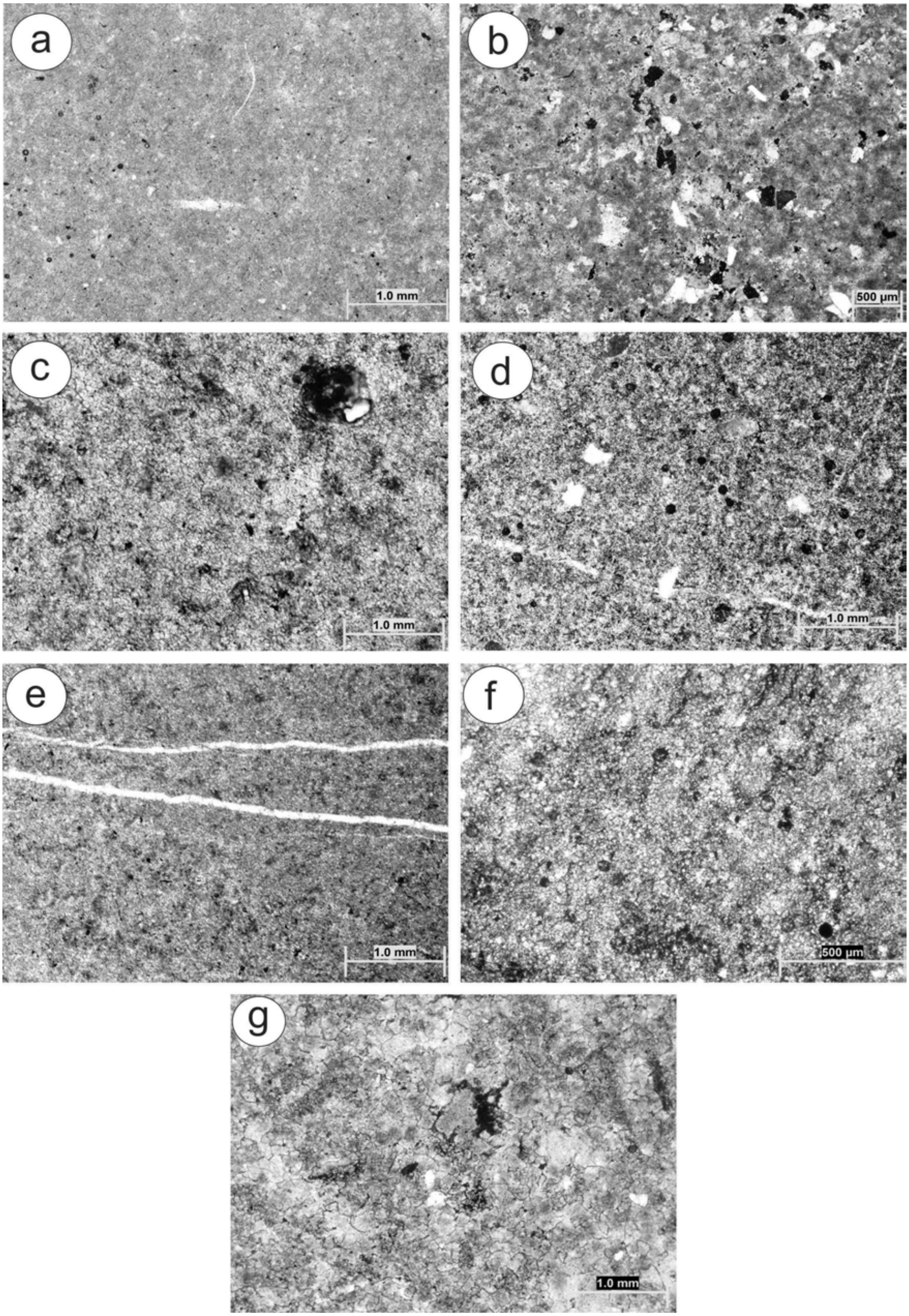

Fig. 6. Field and photomicrographs of the carbonate facies of the Khan Formation in FA1 and FA2. (a) Lime mudstone, (b) Sandy mudstone, (c) Dolomudstone, (d) Sandy Dolomudstone, (e) Dolomicrite, (f) Dolomicrosparite, (g) Dolosparite.

the recrystallization of dolomicrites under critical temperatures (less than 60 °C; Gregg & Shelton 1990). The dolosparites are formed and replaced the limestones at very high temperatures during deep burial diagenetic stages (Gregg & Sibley 1984; Sibley & Gregg 1987; Gregg 1988; Gregg & Shelton 1990).

Interpretation: A shallow subtidal, intertidal to a locally supratidal depositional environment for FA1 is indicated by the dominance of the lime mudstone, sandy lime mudstone, dolomudstone and sandy dolomudstone. The low diversity of fossil assemblages dominated by bivalves, suggests restricted conditions (Colombié & Strasser 2005; Flügel 2010). The overall fine grain-size sediments indicate that the deposition has taken place in a low-energy environment with fluctuating conditions such as tidal flats and restricted lagoons. Based on the fine-grained nature of the dolomite, the absence of skeletal grains and the presence of more than 10 % to 15 % of quartz grains in sandy dolomudstones and sandy mudstone, the FA1 was formed under near-surface low temperature conditions (Gregg & Shelton 1990; Hopkins 2004; Machel 2004) and deposition occurred in a low-energy, restricted intertidal and supratidal environment (Wilmsen et al. 2010; Bayet-Goll et al. 2014; Nowrouzi et al. 2015).

5.2. Lagoonal facies association (FA2) (inner ramp)

Lagoonal facies association in the Khan Formation comprises thin/medium- to thick-bedded wackestones to packstones. Bioclasts in this facies association include green algae, gastropods, ostracods and foraminifers, especially miliolids and fusulinids. Non-skeletal grains are peloids and quartz. Facies association are divided into six facies according to the frequency, the type of carbonate grains and the matrix between carbonate grains. These facies are described as follow.

MF6: Bioclastic wackestone/packstone: This facies comprises of thin- to medium-bedded, dark to light gray beds. The main bioclasts of this facies belong to the typical assemblages of lagoons such as foraminifers, especially fusulinids and miliolids (2–10 % and ranges between 0.1 to 0.7 mm), bivalves (2–15 % and ranges between 0.3 to 1 mm), green algae (1–5 % and ranges between 0.3 to 0.5 mm), echinoderms (5–10 % and ranges between 0.2 to 1 mm) and brachiopods (3–10 % and ranges between 0.4 to 1 mm) (Fig. 7a). Most of the bioclasts are well-preserved and not rounded. The non-skeletal fragments include peloids and quartz which are minor (less than 4 to 5 %). The sizes of peloids range between 0.1 and 0.5 mm; moreover, they are subspherical and subangular, but they are mostly rounded and show moderate to good sorting.

MF7: Peloid bioclastic wackestone/packstone (floatstone/rudstone): This facies is characterized by medium-bedded dark gray limestones. Peloids are the major grain type in this facies (about 15 % to 20 %). The size of peloids ranges between 0.1 and 0.5 mm. Peloids are subspherical, subangular; however, they are mostly rounded and show a moderate sorting. 20–40 % skeletal grains form of this facies encompass bivalves (3–5 % and size ranges between 0.2 to 0.5 mm), echinoderms (5–10 % and size ranges between 0.2 to 3.5 mm), brachiopods (2–5 % and size ranges between 0.2 to 0.8 mm) and gastropods (1–3 % and size ranges between 0.2 to 0.4 mm) that are loosely to closely packed with a poor sorting (Fig. 7b). The grains scattered in the matrix and in some beds form a densely packed grain-supported fabric.

MF8: Fusulinid bioclastic wackestone/packstone (floatstone/rudstone): This facies consists of light gray, thin to medium limestone beds with well-preserved fusulinids (20–45 % and size ranges between 0.8 to 3 mm), brachiopods (2–5 % and size ranges between 0.3 to 1 mm) and echinoderms (5–10 % and size ranges between 0.2 to 1.2 mm) that form 30–60 % of this facies. Minor components are smaller foraminifers (1–2 % and size ranges between 0.1 to 0.3 mm), gastropods (2–3 % and size ranges between 0.2 to 0.8 mm) and ostracodes (1–2 % and size ranges between 0.1 to 0.6 mm) (Fig. 7c, d).

MF9: Peloid packstone: This facies consists of light gray medium beds of poorly to moderately sorted, angular to subrounded peloids (about 40 to 45 %) ranging from 0.1 to 0.3 mm in diameter. Besides, minor constituents are bivalves and rounded muddy intraclasts (about 3 to 4 % and size ranges between 0.2 to 1 mm) scattered in the matrix (Fig. 7e).

MF10: Sandy peloidal wackestone/packstone: This facies is characterized by fine-grained, gray, medium- to thick-bedded limestones. Peloids are dominant components (about 10–35 %); their sizes range between

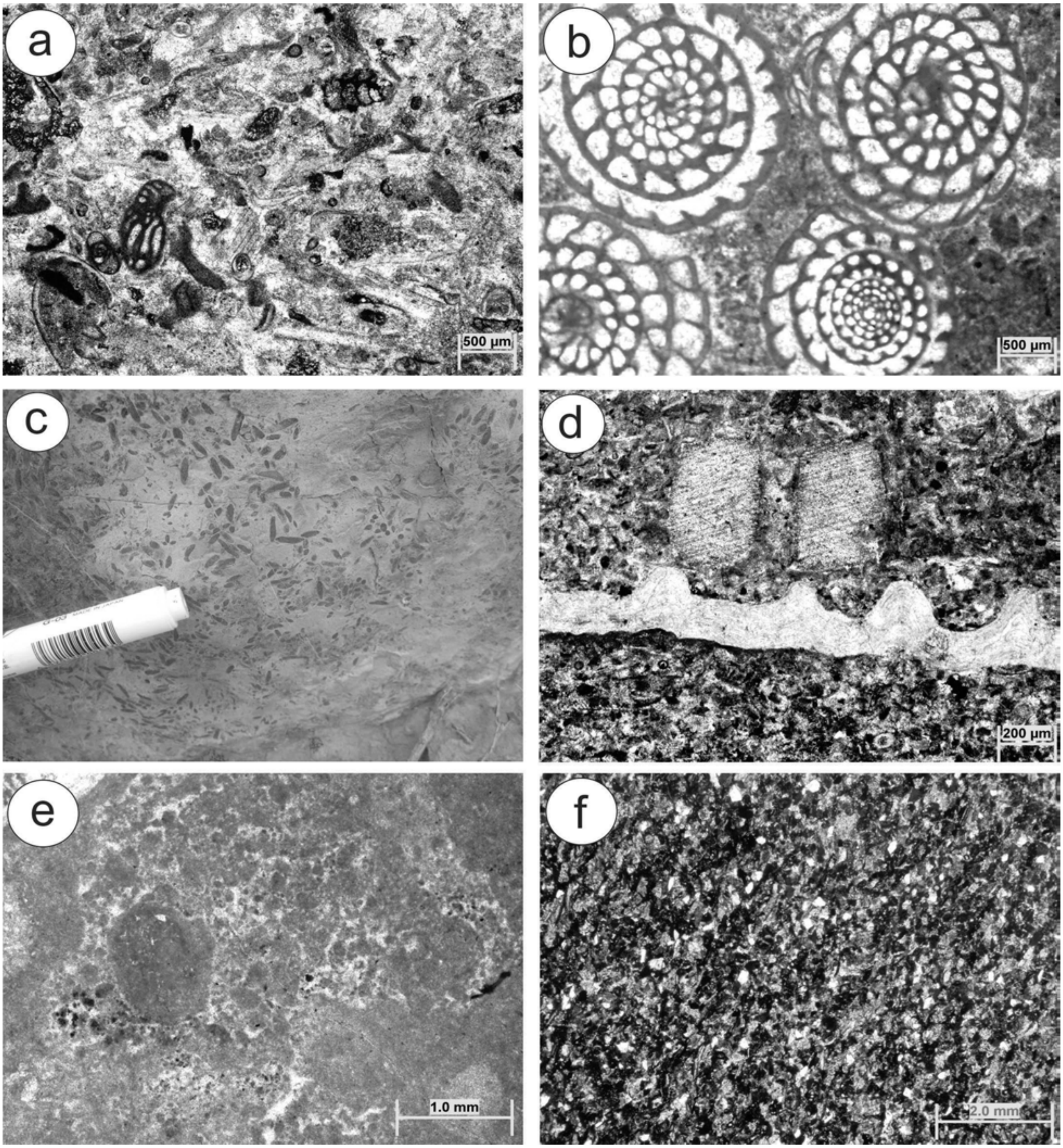

Fig. 7. Field and photomicrographs of the carbonate facies of the Khan Formation in FA2: (a) Bioclastic wackestone/packstone contains benthic foraminifers, bivalves and echinoderms from FA2; moreover, skeletal grains and sparry calcites are replaced by dolomite in some places, (b) Peloid bioclastic wackestone/packstone (floatstone/rudstone) from FA2 contains brachiopods, echinoderms and peloids, (c) Outcrop photograph of the fusulinid bioclastic wackestone/packstone (floatstone/rudstone) in the middle member of the Rahdar section, (d) Fusulinid bioclastic packstone/rudstone, (e) Peloid packstone from FA2 with peloids and muddy intraclasts, (f) Sandy peloidal packstone from FA2 with peloids and sand-sized quartz.

0.1 and 0.5 mm; moreover, they are subspherical, subangular, but mostly rounded and indicate low to moderate sorting. The minor constituents are bivalves (about 3 to 4 % and size ranges between 0.2 to 0.8 mm) and sandy quartz (about 10 %) scattered in the matrix (Fig. 7f).

MF11: Bivalve bioclastic wackestone/packstone (rudstone): This facies is composed of gray medium to thick beds and in places laminated wackestones/packstones. It consists of bivalves (about 20 to 45 %) ranging in size from 0.5 to 3 mm, and displays relatively irregular elongated shapes. Gastropods (about 3 to 5 % and size ranges between 0.2 to 1 mm), bryozoans (about 2 to 5 % and size ranges between 0.2 to 0.6 mm) and small foraminifers (about 1 to 3 % and size ranges between 0.2 to 0.4 mm) are other skeletal grains which scattered in the micrite (Fig. 8a). In some beds they form a densely-packed grain-supported fabric (Fig. 8b).

Interpretation: In FA2, the relatively low abundance and low diversity of a normal marine fauna, the high proportion of micritic mud as well as the partial micritization of skeletal fragments suggest deposition in a low energy and calm environment (Wilson 1975; Hine 1977; Nichols 2000; Fürsich et al. 2003; Srivastava & Singh 2017; Banerjee et al. 2018). The peloidal bioclastic wackestones-packstones indicate widespread low-energy, somewhat restricted peritidal environments and punctuated lagoonal environments (Fürsich et al. 2003). The textural characteristics, the dominance of fusulinids, miliolids, bivalves, gastropods, green algae, and the presence of some micritized grains demonstrate a very shallow-marine backshoal environment, which represents a semi-restricted lagoon in close vicinity of tidal flats with relatively low currents (Romero et al. 2002; Badenas & Aurell 2010) where large fluctuations in salinity and temperature may have occurred (Martini et al. 2007). In the non-laminated wackestones/packstones, the dominance of peloids and the low diversity of bioclasts suggest deposition on an inner ramp (Martini et al. 2007). The co-occurrence of miliolids represents a semi-restricted lagoon (Martini et al. 2007; Palma et al. 2007; Flügel 2010; Vaziri-Moghaddam et al. 2010). Based on these interpretations, this facies association was deposited in a semi-restricted lagoon with an open marine circulation under a low to moderate energy near shoals.

5.3. Bioclastic shoal facies association (FA3) (inner ramp)

This facies association is made up of gray, thin- to thick-bedded limestones. Skeletal limestones, including floatstone, grainstone and packstone facies comprise bioclasts such as echinoderms, corals, *Tubiphytes*, brachiopods, bryozoans, sponge spicules, bivalves and non-skeletal carbonate grains such as ooids, peloids, intraclasts, and quartz.

MF12: Coral framestone: This facies consists of a gray, coarse-grained, thick-bedded coral limestone. In this facies, the colonies of rugose and tabulate corals formed patch reefs. This facies is characterized by solitary and platy colony corals embedded in a sparite calcite and micrite (Figs. 8c, d). Bryozoans are another type of bioclasts which make up about 5–10 %.

MF13: Echinoderm bioclastic grainstone-rudstone: This facies consists of gray to dark gray, thick-bedded limestone with cross lamination. This facies is mostly composed of echinoderms (about 35 to 50 % and size ranges between 0.5 to 4 mm) and other bioclasts such as bivalve fragments (about 1 to 5 % and size ranges between 0.2 to 0.7 mm), bryozoans (about 5 to 15 % and size ranges between 0.5 to 2 mm) and brachiopods (about 2 to 5 % and size ranges between 0.5 to 0.8 mm) which exhibit planar and trough cross lamination (Fig. 8e, f). In some areas, skeletal grains have close packing producing dissolution-compaction structures such as stylolites; furthermore, some echinoderms are surrounded by syntaxial cement.

MF14: Bryozoan bioclastic grainstone/rudstone: This facies consists of a gray, thin- to medium-bedded, coarse-grained limestone (Fig. 9a). Bryozoans are the major grain type in this facies (about 20 to 40 % and size ranges between 0.5 to 4.5 mm) (Fig. 9b). Other bioclasts are represented by corals (2 to 5 % and size ranges between 0.5 to 0.8 mm), bivalves (2 to 3 % and size ranges between 0.3 to 0.5 mm), fusulinids (2 to 5 % and size ranges between 0.5 to 1.2 mm) and echinoderms (2 to 5 % and size ranges between 0.3 to 0.7 mm). In this facies non-skeletal grains are minor components which consist of ooids (1 to 2 % and size ranges between 0.1 to 0.3 mm) and rounded muddy intraclasts (about 1 to 2 % and size ranges between 0.2 to 0.6 mm).

MF15: Intraclastic grainstone: This facies is a gray to light gray, thin- to medium-bedded, composed of

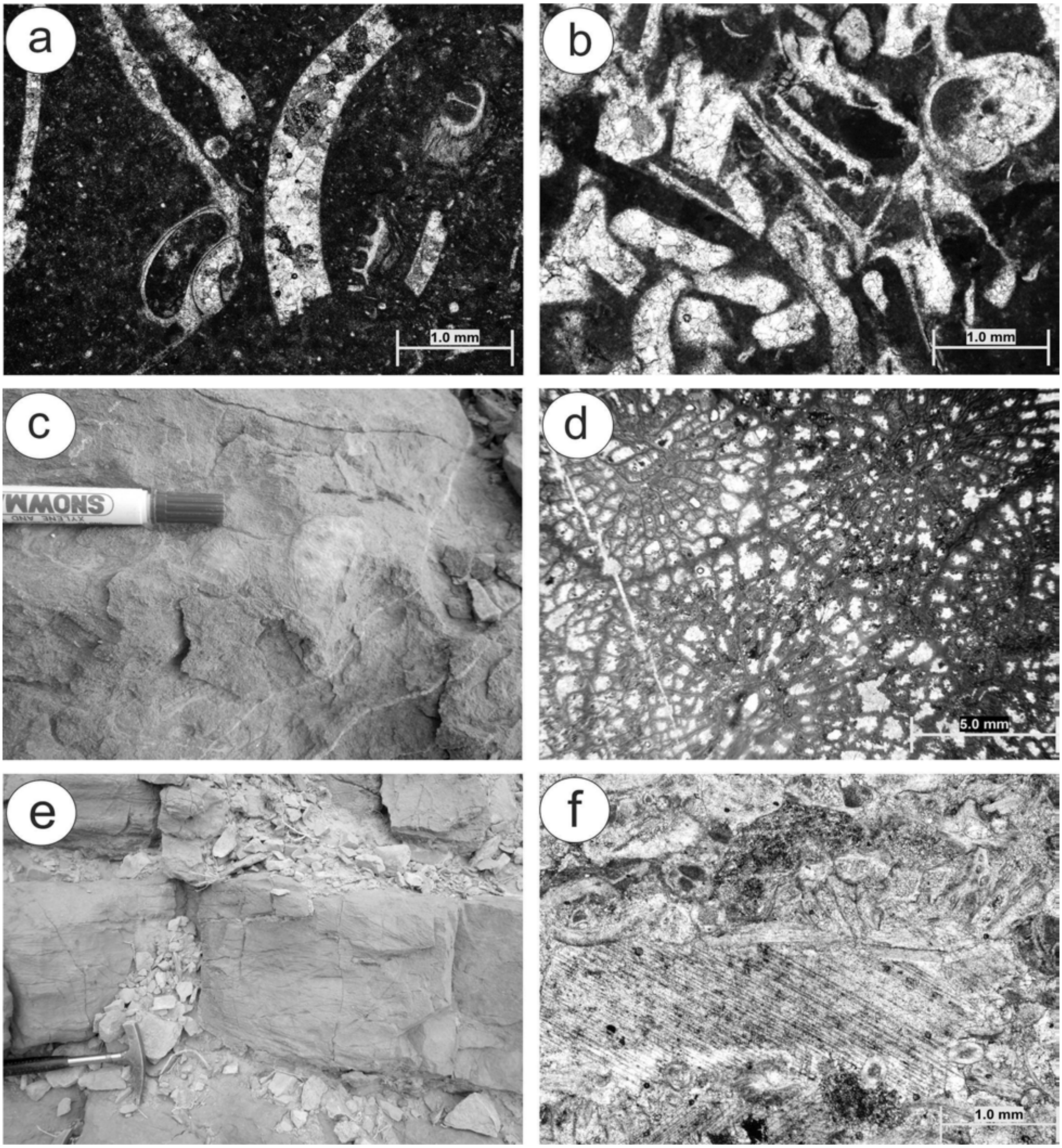

Fig. 8. Field and photomicrographs of the carbonate facies of the Khan Formation in FA2 and FA3. (a, b) Bivalve bioclastic wackestone/packstone (rudstone) in micrite with bivalve fragments, gastropods, echinoderms and bryozoans, (c) Outcrop photograph of the coral framestone: the rugose and tabulate colony of corals have constructed a patch reef in the lower member of the Bakhshi section, (d) Coral framestone facies in FA3, (e) Outcrop photograph of the echinoderm bioclastic grainstone-rudstone with planar and trough cross-lamination in the middle member of the Bakhshi section, (f) Echinoderm bioclastic grainstone-rudstone facies in FA3 with echinoderms, bryozoans and skeletal grains.

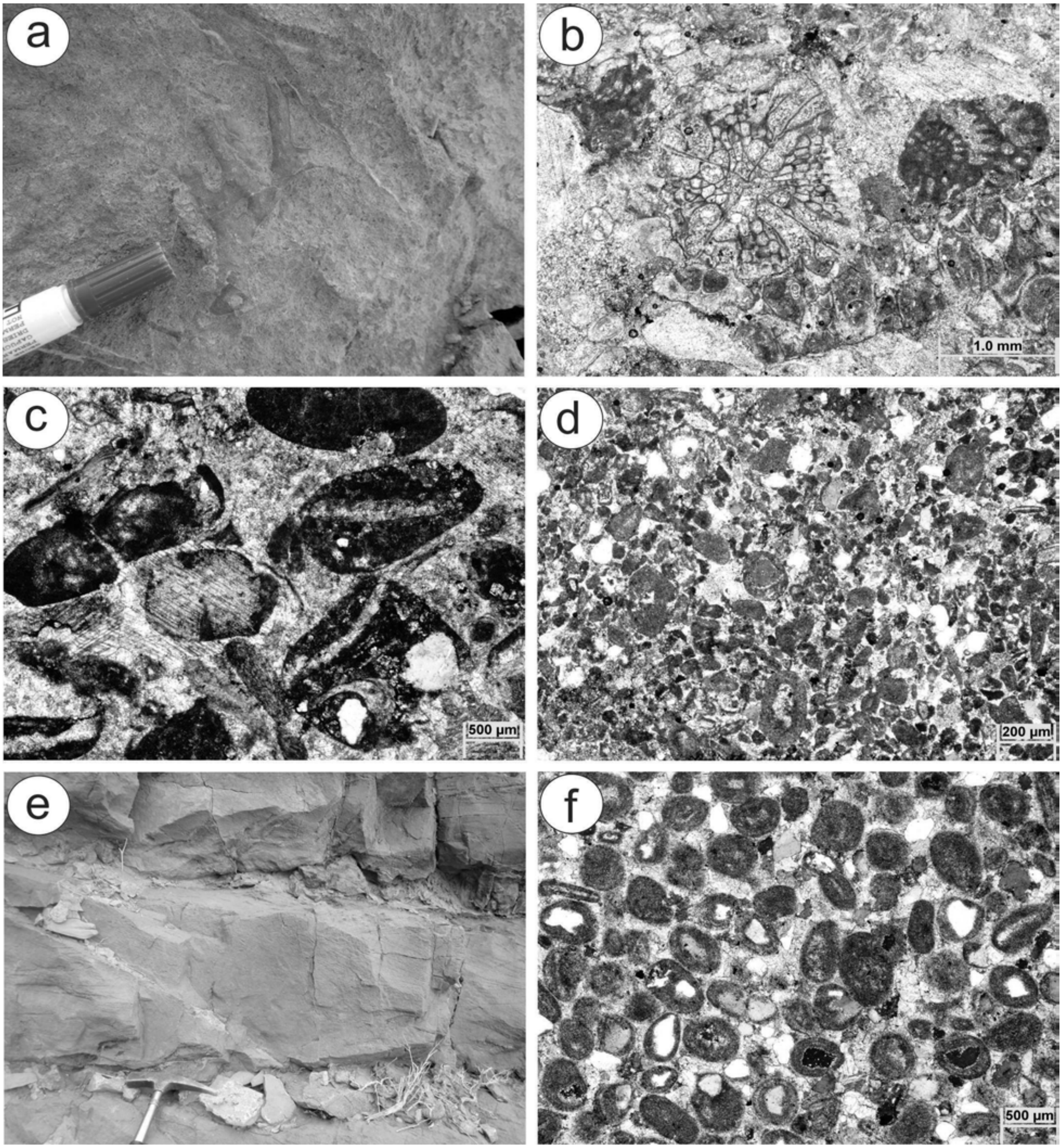

Fig. 9. Field and photomicrographs of the carbonate facies of the Khan Formation in FA3. (a) Outcrop photograph of the bryozoan bioclastic grainstone/rudstone in the middle member of the Tangal-e-Shotoru section, (b) bryozoan bioclastic grainstone/rudstone facies with bryozoans and fusulinid fragments in FA3, (c) Intraclastic grainstone with intraclasts and echinoderms. The intraclasts contain bivalves, brachiopod fragments and quartz, (d) Sandy ooid peloidal grainstone–packstone facies in FA3, (e) Outcrop photographs of the ooid grainstone with trough and planar cross-laminations in the middle member of the Rahdar section, (f) Well-sorted ooid grainstone with quartz nuclei.

muddy intraclasts (20 to 40 %) which range in size from 0.5 to 2 mm. Besides, they display rounded and moderately sorted components (Fig. 9c), which contain bivalves, brachiopods and quartz fragments. Echinoderms are another component in this facies (about 5 to 8 % and size ranges between 0.2 to 0.7 mm).

MF16: Sandy ooid-peloidal packstone-grainstone: This facies consists of thinly-bedded, dark gray limestone. Peloids are the major non-skeletal carbonate grain type (25–30 %) which are spherical to elongated and range from 0.05 to 0.1 mm in diameter. Ooids which range from 0.1 to 0.3 mm in diameter, are another non-skeletal carbonate grain (10–15 %) that are sorted and subrounded. The minor constituent is sandy quartz (about 10–12 %) (Fig. 9d).

MF17: Oolitic grainstone: This facies consists of a light gray, medium-bedded, fine- to coarse-grained oolitic grainstone with planar and trough cross lamination (Fig. 9e). The moderately to well-sorted ooids with quartz nuclei form 85 % of this facies (size ranges between 0.3 to 0.6 mm). Some of ooids exhibit poorly preserved concentric structures due to the dolomitization process (Fig. 9f).

MF18: Intraclastic ooid grainstone: This facies forms thin- to medium-bedded, light to gray beds composed of moderately sorted ooids (35–40 % with size ranges between 0.3 to 0.8 mm) and broken intraclasts (20 % and size ranges between 0.3 to 1.1 mm) which contain ooids and bivalves surrounded by sparry cement (Fig. 10a). The bioclasts such as smaller bryozoans (2–3 % with size ranges between 0.2 to 0.5 mm) and echinoderms (3–5 % with size ranges between 0.3 to 0.6 mm) are present as minor components.

MF19: Bioclastic packstone/grainstone (rudstone/floatstone): This facies consists of dark gray, medium-bedded packstones/grainstones. The skeletal grains include brachiopods (15–20 % with size ranges between 0.8 to 2 mm), bryozoans (15–20 % with size ranges between 0.5 to 3 mm) and echinoderms (3–5 % with size ranges between 0.3 to 0.6 mm) (Fig. 10b). Not only allochems are cemented by sparry calcite, but some of them (echinoderms) are surrounded by syntaxial cement.

MF20: Sandy ooid bioclastic packstone/grainstone: This facies is a gray to light gray, thin- to medium-bedded grainstone to packstone. This facies is dominated by bioclasts such as bryozans (15–20 % with size ranges between 1.2 to 2.5 mm), echinoderms (5–8 % with size ranges between 0.3 to 0.6 mm), green algae (1–3 % with size ranges between 0.2 to 0.5 mm) and gastropods (1–2 % with size ranges between 0.3 to 0.4 mm). Ooids (about 10 % with size ranges between 0.3 to 0.5 mm) and muddy intraclasts (3–5 % with size ranges between 0.3 to 0.6 mm) are as non-skeletal carbonate grains. Fine to coarse-grained, moderate to well-sorted, sub-angular to sub-rounded monocrystalline quartz grains represent about 10 % to 15 % of the rock. This microfacies is characterized by the micritic matrix cemented by sparry calcite (Fig. 10c).

MF21: Bioclast intraclastic packstone/grainstone: This facies is a gray to light gray, thin- to medium-bedded limestone dominated (up to 20 %) by large intraclasts (from 1 to 3 mm), which contain bryozoans, echinoderms and brachiopod fragments enveloped by micrite. The clasts are well-rounded and well-sorted with spherical to elongated forms. Echinoderms (5–10 % with size ranges between 0.3 to 0.7 mm), bryozoans (3–5 % with size ranges between 0.3 to 0.8 mm), green and red algae (5–10 % with size ranges between 0.3 to 0.6 mm), bivalves and ostracods (2–3 % with size ranges between 0.3 to 0.6 mm) are skeletal components in this facies. This microfacies is characterized by a micritic matrix cemented by equigranular calcite crystals; moreover, some echinoderms are surrounded by syntaxial cement (Fig. 10d).

MF22: *Tubiphytes* bioclastic packstone/rudstone: This facies is composed of thin-bedded, light to dark gray *Tubiphytes* bioclastic packstone/rudstone and contains both heterozoan (sponge spicules (5–15 % and size ranges between 0.05 and 0.2 mm), bryozoans and brachiopods (totally 5 % with size ranges between 0.2 and 0.8 mm)) as well as photozoan elements (*Tubiphytes* with 15–35 % abundance and size ranges between 0.2 and 1 mm). The components are enveloped by micrite and sparry calcite (Fig. 10e).

Interpretation: The abundance and high diversity of skeletal fauna (such as echinoderms, bryozoans, brachiopods, and bivalves) suggest high-energy reworking and deposition in a barrier setting that can be differentiated this facies from facies in supratidal, intertidal, and restricted platform areas (Novak et al. 2013; Srivastava & Singh 2017). The presence of ooids and peloids in MF16 with a grainstone texture suggests the reworking of grains from nearby the fair-

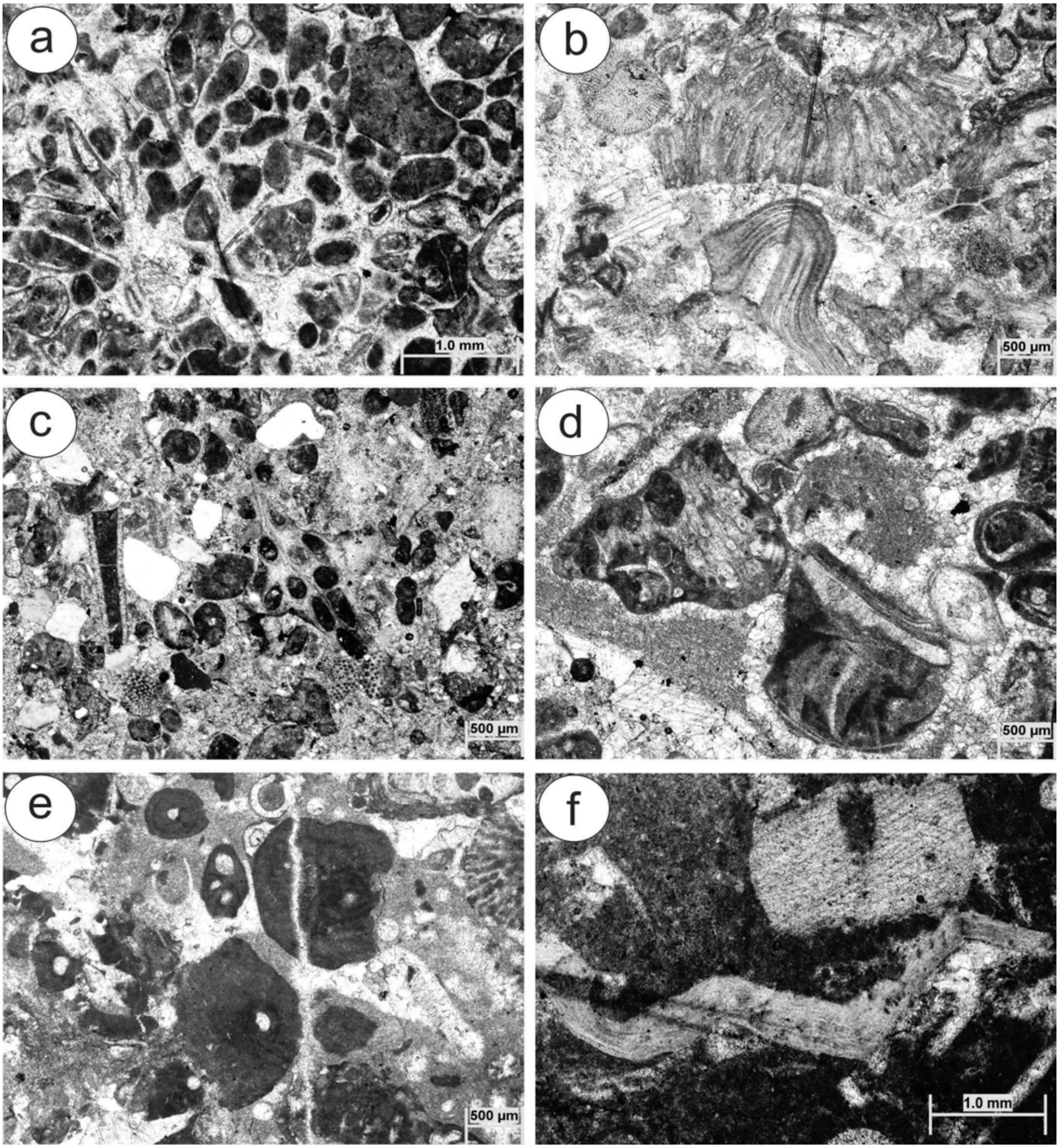

Fig. 10. Field and photomicrographs of the carbonate facies of the Khan Formation in FA3 and FA4: (a) The intraclastic ooid grainstone contains well-sorted ooids, muddy intraclasts and intraclast with bryozoan fragments, (b) Bioclastic packstone/grainstone (rudstone/floatstone) with bryozoans, brachiopods and echinoderms, (c) Sandy ooid bioclastic packstone/grainstone with bryozoans, echinoderms, gastropods, ooids and sandy quartz in FA3, (d) bioclast intraclastic packstone/grainstone with intraclasts, bryozoans, echinoderms and ostracodes in FA3. The intraclasts contain bivalves, bryozoans and brachiopod fragments, (e) *Tubiphytes* bioclastic packstone/rudstone with *Tubiphytes*, sponge spicules and bryozoans in FA3. (d) Bioclastic wackestone/packstone facies of a shallow open marine environment (FA4).

weather wave base (Bertola et al. 2013). The presence of photozoan elements such as corals and *Tubiphytes* may reflect oligotrophic conditions which confirm warm and shallow water environment above the FWWB (Hallock & Glenn 1986). The existence of fully preserved colonies of corals and bryozoans with residual growth and branched Rugosa indicate a shallower and warm environment near the FWWB. The presence of cross lamination in MF13 and MF17 suggests deposition in relatively high energy shoal environments with normal marine conditions (Cortes et al. 2009; Banerjee et al. 2018). The ooid grainstone indicates a high energy environment that has been subjected to constant wave agitation and produced a well-sorted grainstone (Flügel 2010; Tucker & Wright 1990). The intraclastic ooid grainstone implies deposition in the highest energy portion of a seaward shoal within the surf zone. The presence of grain-supported and mud-free (or lesser amounts of mud) textures in the bioclastic rudstone/floatstone indicate that wave and current activity occurred in a high energy depositional environment, i.e., bioclastic shoals developed in a seaward shoal environment. The bioclast intraclastic grainstone was deposited in a high energy, upper intertidal sub-environment supported by the lack of micrites (Shinn 1983). In MF23, the presence of bryozoans, brachiopods and siliceous sponge spicules are interpreted as mid-ramp (shallow open marine) elements immigrating into inner ramp (shoal) areas due to an underlying cooling from warm to subtropical (warm temperate) conditions. A similar biotic composition has been observed in the Canadian Arctic (Sverdrup Basin) by Reid et al. (2007) and Bensing (2007) within the late Sakmarian to earliest Artinskian Raanes Formation, representing inner- to middle ramp areas.

5.4. Shallow open marine facies association: mid-ramp (FA4)

The shallow open-marine facies association is mainly composed of gray, thin bedded wackestones/packstones. Facies association FA4 contains only one facies including bioclastic wackestones/packstones as described below.

MF23: Bioclastic wackestone/packstone: This facies consists of gray to dark gray, thin-bedded limestone. The skeletal grains consist of echinoderms (10–20 % with size ranges between 0.2 to 1.5 mm), brachiopods (1–5 % with size ranges between 0.3 to 1 mm), bivalves (1–5 % with size ranges between 0.3 to 1 mm) and small foraminifers (1–5 % with size ranges between 0.3 to 0.5 mm) (Fig. 10f) surrounded by micrite.

Interpretation: This facies association is not found extensively in the Khan Formation. The presence of thin bedding in bioclastic wackestones/packstones is characteristic for low rates of sedimentation and low-energy depositional environment. This facies was deposited in the shallower part of an open marine environment (Arefifard & Isaacson 2011). Skeletal fragments such as brachiopods and echinoderms are common in the middle ramp environment in both shoal and open marine (Pomar 2001a; Pomar 2001b; Cosovic et al. 2004; Martini et al. 2007; Sardar Abadi et al. 2017). The abundance of carbonate mud and the poorly sorted grains in this facies association is indicative of a quiet-water and low-energy environment (Arefifard & Isaacson 2011; Sardar Abadi et al. 2017). Hence, an open marine environment is likely for this facies.

6. Discussion

6.1. Depositional model

Five facies (A to E) were recognized in siliciclastic successions which represent depositional environments ranging from proximal lower shoreface, middle shoreface, upper shoreface, foreshore, tidal inlet and washover fan/lagoon. The seaward progradation of shoreline produced coarsening-upward packages in the siliciclastic deposits of Khan Formation which indicates an upwards increase in depositional energy (Fig. 3). Coarsening and thickening upward successions are interpreted as a prograding shoreface/foreshore system (Fig. 11a). It appears that the energy level was sufficient for the transport and deposition of sand as well as gravel, and the prograding of a shoreface/foreshore system during the deposition of the Khan Formation. The facies distributions indicate that the barrier margin of the lagoon was influenced by storm washover sand destruction of the barrier, which was apparently the main source of sandy sediment to the lagoon. The development of the barrier may have been aided by the influx of sediment by an earlier sea-level fall and the reworking into barriers during the subsequent transgressions (Stapor & Stone 2004). A generalized model which illustrates

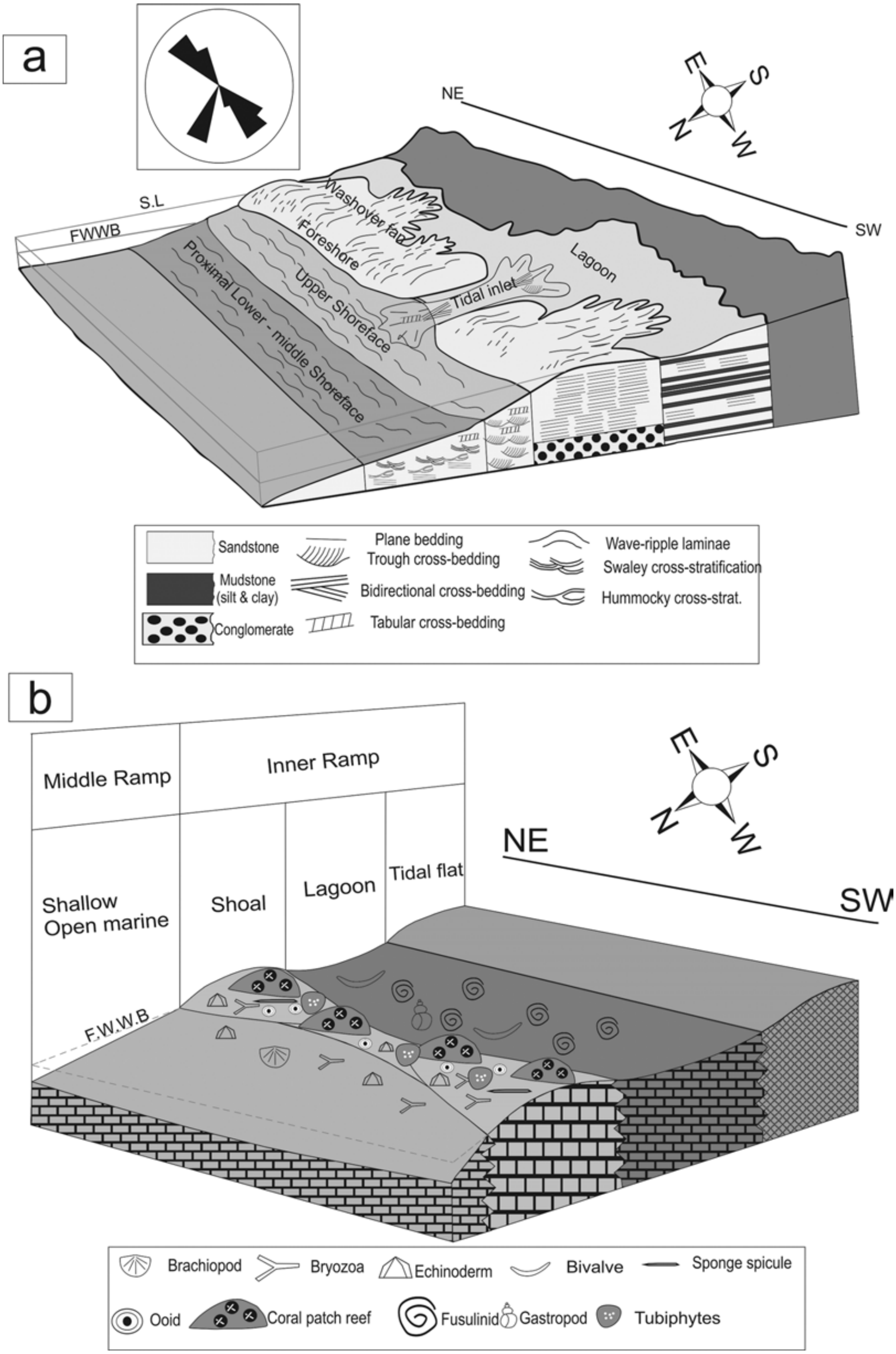

Fig. 11. Schematic depositional models of the Khan Formation: (a) siliciclastic successions of the Khan Formation show onshore-offshore facies gradients related to palaeoenvironments of the siliciclastic deposits; (b) carbonate successions of the Khan Formation indicating a homoclinal ramp, which mainly consists of the inner and middle ramp sub-environment. FWWB = fair-weather wave base.

the main depositional environments of the siliciclastic successions is shown in Fig. 11a. Based on the continuous outcrops of the Khan Formation, we reconstructed the sedimentary environment of the carbonate successions using skeletal and non-skeletal components, sedimentological features as well as the matrix grain-size. Based on the absence of oncoids, cortoids, aggregate grains and large barrier reefs and the presence of vast areas of tidal flats and the low abundance of open marine carbonates, we consider the carbonate successions were deposited on a homoclinal carbonate ramp (Read 1985). The previous work confirms this depositional environment for the Khan Formation deposits (Shadan & Hosseini-Barzi 2010; Arefifard & Isaacson 2011; Shahraki et al. 2015; Emraninasab et al. 2016; Emraninasab et al. 2017). Four facies associations are identified comprising tidal flats, lagoons, shoal and shallow open marine environments which developed in the inner and middle ramp. The most important criteria of tidal flat conditions in the fine crystalline dolomites are the fine grain nature and the presence of detrital quartz. The textural features and dominance of fusulinids, miliolids, bivalves, gastropods and the presence of some micritized grains indicate a very shallow-marine back-shoal environment. It represents a semi-restricted lagoon in close vicinity of tidal flats with relatively low currents (Romero et al. 2002; Badenas & Aurell 2010), where large fluctuations in salinity and temperature may have occurred (Martini et al. 2007). The high energy inner-ramp (shoal) is characterized by the appearance of non-skeletal carbonate grains like peloids, ooids and intraclasts and skeletal grains like echinoderms, bryozoans, corals and *Tubiphytes* in a grainstone/rudstone to packstone texture (Testa & Bosence 1998; Sardar Abadi et al. 2017). The shallow marine facies association is not widespread in the Khan Formation. As a result, the carbonate successions of the Khan Formation represent a homoclinal ramp with a wide inner and mid-ramp as shown in Fig. 11b.

6.2. Depositional sequences

The Lower Permian (late Sakmarian to early Artinskian) Khan Formation in the Kalmard sub-basin displays a cyclic sequence (Fig. 3) which can be divided into third-order shallowing-upward depositional sequences. On the basis of facies relationships and the recognition of key surfaces in the Khan Formation, four (in the Bakhshi and Bibisene sections) and three depositional sequences (in the Tangal-e-Shotoru and Rahdar sections) are recognized which are composed of lowstand, transgressive and highstand systems tract. Each sequence records a transgression and a regression.

Sequence 1 was deposited in all sections. The LST deposits of the sequence 1 include siliciclastic deposits which also occur in the lower part of the TST. The LST succession contains a lower/middle shoreface to foreshore facies which shows a coarsening-upward trend in all sections. The transgressive system tract in sequence 1 is composed mainly of siliciclastic (in the lower part of the TST) and carbonate successions which start with lower/middle shoreface (in the Bibisene section), upper shoreface (in the Bakhshi and Tangal-e-Shotoru sections) and tidal inlet (in the Rahdar section) as transgressive surface (TS), and then in a deepening-upwards trend it ends with a shallow open marine carbonate facies (bioclastic wackestone/packstone) as maximum flooding surface (mfs). The HST deposits are recognized by a shallowing-upward progradational stacking pattern, which mostly includes lagoonal and tidal flat facies with more restricted faunas. The lower and upper boundaries of sequence 1 in the Rahdar section are both of type 1 (because of a disconformity with the Gachal Fm. in the lower boundary and the presence of a bauxite/laterite horizon in the upper boundary) and in the others are of type 1 and type 2, respectively (Fig. 3).

Like sequence 1, sequence 2 starts with LST sedimentary deposits composed of sandstones (foreshore facies in the Rahdar section and lower/middle shoreface in the others) at the beginning of LST and mudstones (shale and siltstone) at the end of it, except in the Tangal-e-Shotoru section, which ends with foreshore sandstones. Siliciclastic deposits continued in the lower part of the TST as transgressive surface in the Tangal-e-Shotoru and Bibisene sections. The TST is characterized by alternating carbonates of lagoon and barrier facies. This deepening-upward trend ends with shallow open marine carbonate facies (bioclastic wackestones/packstones) as maximum flooding surface (mfs) in all sections except Tangal-e-Shotoru which is ended by barrier carbonates (mfs). The HST is marked by fusulinid-rich beds. The transition from barrier to mainly lagoonal and tidal flat facies indicates a sea-level fall, gradual shallowing conditions, and a reduced accommodation space during the HST. The upper boundary of sequence 2 is type 2 (SB2) in the Tangal-e-Shotoru and Rahdar sections and type 1

(SB1) in the Bakhshi and Bibisene sections because of bauxite/laterite horizons (Fig. 3).

Sequence 3 was deposited in the Bakhshi and Bibisene sections completely, but in the Tangal-e-Shotoru and Rahdar sections it is only composed of LST siliciclastic deposits. The LST deposits start with sandstones (lower/middle shoreface to washover fan facies), which gradually change upwards to alternating sandstone and mudstone (washover fan/lagoon facies). At the top of LST, the appearance of a bauxite/laterite horizon in the Tangal-e-Shotoru and Rahdar sections marks the end of the sedimentation of the Khan Formation in these sections.

The TST in the Bakhshi and Bibisene sections is characterized by alternating carbonates of tidal flats, barriers and lagoons with a general deepening-upward trend ending in barrier carbonates (dolomitized ooid grainstone facies in the Bakhshi section and dolomitized echinoderm bioclastic packstone/grainstone facies in the Bibisene section) as maximum flooding surface. The HST is thin and composed of lagoonal (in the Bibisene section) and tidal flat facies (in the Bakhshi section). The upper boundary of the sequence 3 is type 2.

Sequence 4 is represented in Bakhshi and Bibisene sections and only composed of LST. This sequence starts with coarse-grain sandstones of the upper shore face and foreshore which gradually change to alternating sandstones and mudstones of a washover fan/lagoonal facies. The upper boundary of the sequence 4 with the Lower Triassic Sorkh Shale Formation is SB1.

The upper boundary of the Khan Formation shows a significant disconformity, which is related to epeirogenic movements at the end of the Sakmarian to the early Artinskian stages. This disconformity is widespread and very useful for correlation. After the deposition of the Khan Formation, the Kalmard Sub-Block has experienced a significant regression. From the late Early Permian through Early Triassic times, this area was subaerially exposed, as evidenced by the bauxite horizons on top of the Khan Formation (Arefifard & Isaacson 2011).

The stratigraphic architecture of the Khan deposits are the result of the interplay between regional uplift caused by the Kalmard Fault and relative sea-level changes. Fault-driven subsidence and the continuous creation of accommodation in the hangingwall of the Kalmard Fault led to marked spatial variability in stratal stacking patterns, systems tracts and key stratal surfaces (Bayet-Goll et al. 2018).

6.3. Palaeogeography

The similarity between most Iranian Palaeozoic deposits to their counterparts in the Arabian Plate confirmed the idea that Iran was part of Gondwana during the Late Palaeozoic (Stöcklin 1968; Berberian & King 1981). Following the opening of Neo-Tethys, Iran with other Cimmerian terranes, including Turkey, Afghanistan, Karakoram, Tibet, and Qiangtang rifted away from Gondwana in Early Permian times, and moved northward across Palaeo-Tethys Ocean; finally it collided with the Eurasian margin which created the Eo-Cimmerian Orogeny (Ruban et al. 2007; Muttoni et al. 2009a; Muttoni et al. 2009b; Zanchi et al. 2009;Berra & Angiolini 2014). Besides, the Permian Period recorded a drastic palaeoclimatic change from a global icehouse in the Carboniferous–early Cisuralian (Lower Permian) towards a greenhouse state in the Lopingian (Late Permian) (Fielding et al. 2008; Shi & Waterhouse 2010; Arefifard 2017).

In the Khan Formation sections, the evidence such as the presence of bauxite/laterite horizons, highly mature quartz grains and plant fossils in siliciclastic successions and the presence of photozoan fauna such as corals and *Tubiphytes* in carbonate deposits indicate that the Khan Formation was deposited in a warm and humid condition. Moreover, Badpa et al. (2014) stated that the colonial corals in the middle part of the Khan Formation in the Rahdar section belong to the Tethyan Realm which was only confined to tropical latitudes of 35 degrees and lived in turbulent shallow water as patch reefs. On the other hand, the presence of a heterozoan fauna, like echinoderms, bryozoans, and sponges in the carbonate successions suggests a cooler climate. Moreover, according to Davydov & Arefifard (2007) fusulinids of the Khan Formation belong to a temperate transitional cool to cold water fauna of higher latitudes. So, there is an alternation of cool to warm and humid climate during the deposition of the Khan Formation (late Sakmarian–early Artinskian) which is consistent with several discrete icehouse times punctuated by warmer periods of glacial minima, and involved in a series of cycles of glaciation/deglaciation during the Permian (Fielding et al. 2008; Bishop et al. 2009). The sea-level highstands of the Lower Carboniferous Gachal Formation changed to lowstands in the lower siliciclastic part of the Khan Formation during the Sakmarian caused by glaciations (Ross & Ross 1988; Ross & Ross 1996; Nakazawa & Ueno 2009).

Decreasing water temperatures and the presence of a cool water fauna like the fusulinids and heterozoan fauna of the Khan Formation are probably caused by the upwelling of cold, nutrient-rich deep waters of higher latitudes cutting off warm-water masses from the Tethys in low latitudes along the southern margin of Gondwana (Blomeier et al. 2011). Higher nutrient and energy levels as well as increased siliciclastic input are probably due to more humid climatic conditions marked by increased precipitation and the uplift of a local siliciclastic source area caused by the Kalmard Fault activity (Bayet-Goll et al. 2018).

This conclusion confirms the recently published results of Arefifard (2017) about deposition of Khan Formation on low latitude setting during late Sakmarian–early Artinskian. Moreover, the previous ideas of Davydov & Arefifard (2007) which states fusulinids of the Khan Formation belong to temperate transitional cool to cold water fauna of higher latitudes is confirm with the upwelling of cold water to low latitude warm water.

7. Conclusions

The detailed study of the Lower Permian Khan Formation in Central Iran (Kalmard Sub-Block) indicates a range of siliciclastic and carbonate environments which frequently changed through time, and consists of conglomerates, sandstones, mudstones, limestones, dolomitic limestones and dolostones. Based on the sedimentological and stratigraphic framework of the Lower Permian Khan Formation, the siliciclastic successions accumulated on a shallow marine environment and include proximal lower-middle shoreface, upper shoreface, foreshore, tidal inlet and washover fan/lagoonal deposits. These successions are thickening and coarsening upward. Thus, the siliciclastic successions of Khan Formation belong to a pragradational barrier island complex. The carbonate facies of the Khan Formation formed on a homoclinal ramp, mostly on the inner and middle ramp, including tidal flats, lagoons, barriers, patch reefs and shallow open marine environments. Horizontal lamination, planar and trough cross-lamination, swaley and hummocky cross-stratification are the most abundant sedimentary structures in the Khan Formation. Sequence stratigraphy studies indicate 3 and 4 depositional sequences (third-ordered sequence) in the Tangal-e-Shotoru, Rahdar and Bakhshi, Bibisene sections, respectively, where each cycle shows a progradation and regression. Based on highly mature quartz grains, the presence of bauxite/laterite and terrestrial plant fossils in the siliciclastic successions, the Khan Formation was deposited under warm and humid conditions.

Acknowledgements

The authors are very thankful to the reviewers Dr. Sakineh Arefifard, Dr. Mahdi Badpa and an anonymous reviewer for very useful comments that improved our manuscript significantly. We also acknowledge the editor-in-chief Dr. Günter Schweigert for making constructive suggestions. Furthermore, we would like to thank Yaghub Nasiri, Mahdi Hadi and Ehsan Zamanian for assisting in the fieldwork.

References

Adabi, M.H. (2004). A re-evaluation of Aragonite versus Calcite seas. Carbonates and Evaporites, **19**(2), 133–141. doi: 10.1007/BF03178476

Aghanabati, A. (1977). Étude géologique de la région de Kalmard (W. Tabas). Geological Survey of Iran, Report No. 35, 230 pp.

Aghanabati, S.A. (2004). Geology of Iran. Tehran: Geological Survey of Iran. (in Persian)

Alavi, M. (1991). Tectonic map of the Middle East. Geological Survey of Iran.

Arefifard, S. (2018). Evidence of warm climate during late Sakmarian–early Artinskian in Posht-e-Badam Block, Central Iran and its paleogeographic implication. Geological Journal, **53**(2), 742–753. doi: 10.1002/gj.2924

Arefifard, S., & Isaacson, P.E. (2011). Permian sequence stratigraphy in east-central Iran: Microplate records of Peri-Tethyan and Peri-Gondwanan events. Stratigraphy, **8**(1), 61–83.

Azhdari, A. (1999). Geological map of the Robat-e-Khan sheet (1:100000). Tehran: Geological Survey of Iran.

Bádenas, B., & Aurell, M. (2010). Facies models of a shallow-water carbonate ramp based on distribution of non-skeletal grains (Kimmeridgian, Spain). Facies, **56**(1), 89–110. doi: 10.1007/s10347-009-0199-z

Badpa, M., Khaksar, K., Ashouri, A., & Badpa, M. (2014). The first report of coral fossils in the Khan Formation (Rahdar section, Kalmard Mountains, E-Iran). 32nd National & 1st International Geosciences Congress.

Banerjee, S., Khanolkar, S., & Saraswati, P.K. (2018). Facies and depositional settings of the Middle Eocene-Oligocene carbonates in Kutch. Geodinamica Acta, **30**(1), 119–136. doi: 10.1080/09853111.2018.1442609

Bayet-Goll, A., Chen, J., Moussavi-Harami, R., & Mahboubi, A. (2015a). Depositional processes of ribbon carbonates in middle Cambrian of Iran (Deh-Sufiyan Formation, Central Alborz). Facies, **61**(9), 1–18. doi: 10.1007/s10347-015-0436-6

Bayet-Goll, A., De Carvalho, C.N., Mahmudy-Gharaei, M.H., & Nadaf, R. (2015b). Ichnology and sedimentology of a shallow marine Upper Cretaceous depositional system (Neyzar Formation, Kopet-Dagh, Iran): Palaeoceanographic inuence on ichnodiversity. Cretaceous Research, **56**, 628–646. doi: 10.1016/j.cretres.2015.07.008

Bayet-Goll, A., Geyer, G., Wilmsen, M., Mahboubi, A., & Moussavi-Harami, R. (2014). Facies architecture, depositional environments, and sequence stratigraphy of the Middle Cambrian Fasham and Deh-Sufiyan Formations in the central Alborz, Iran. Facies, **60**(3), 815–841. doi: 10.1007/s10347-014-0401-9

Berberian, M., & King, G. (1981). Towards a paleogeography and tectonic evolution of Iran. Canadian Journal of Earth Sciences, **18**(2), 210–265. doi: 10.1139/e81-019

Berra, F., & Angiolini, L. (2014). The evolution of the Tethys region throughout the Phanerozoic: a brief tectonic reconstruction. In L. Marlow, C. Kendall, & L. Yose (Eds.), Petroleum systems of the Tethyan region. AAPG Memoirs, 106, 1–27. doi: 10.1306/13431840M1063606

Bertola, C., Boulvain, F., Da Silva, A.C., & Poty, E. (2013). Sedimentology and magnetic susceptibility of Mississippian (Tournaisian) carbonate sections in Belgium. Bulletin of Geosciences, **88**(1), 69–82.

Blomeier, D., Dustira, A., Forke, H., & Scheibner, C. (2011). Environmental change in the Early Permian of NE Svalbard: From a warm-water carbonate platform (Gipshuken Formation) to a temperate, mixed siliciclastic-carbonate ramp (Kapp Starostin Formation). Facies, **57**(3), 493–523. doi: 10.1007/s10347-010-0243-z

Buatois, L.A., & Mángano, M.G. (2011). Ichnology: Organism-substrate interactions in space and time. Cambridge: Cambridge University Press. doi: 10.1017/CBO9780511975622

Catuneanu, O., & Zecchin, M. (2013). High-resolution sequence stratigraphy of clastic shelves II: Controls on sequence development. Marine and Petroleum Geology, **39**(1), 26–38. doi: 10.1016/j.marpetgeo.2012.08.010

Catuneanu, O., Abreu, V., Bhattacharya, J.P., Blum, M.D., Dalrymple, R.W., Eriksson, P.G., … Gibling, M.R. (2009). Towards the standardization of sequence stratigraphy. Earth-Science Research, **92**, 1–33.

Catuneanu, O., Galloway, W.E., Kendall, C.G. S.T. C., Miall, A.D., Posamentier, H.W., Strasser, A., & Tucker, M.E. (2011). Sequence stratigraphy: Methodology and nomenclature. Newsletters on Stratigraphy, **44**(3), 173–245. doi: 10.1127/0078-0421/2011/0011

Cheel, R.J., & Leckie, D.A. (1993). Hummocky cross-stratification. Sedimentology Review, **1**, 103–122. doi: 10.1002/9781444304534.ch7

Coffey, B.P., & Sunde, R.F. (2014). Lithology-based sequence-stratigraphic framework of a mixed carbonate-siliciclastic succession, Lower Cretaceous, Atlantic coastal plain. AAPG Bulletin, **98**(8), 1599–1630. doi: 10.1306/08211312087

Colombié, C., & Strasser, A. (2005). Facies, cycles, and controls on the evolution of a keep-up carbonate platform (Kimmeridgian, Swiss Jura). Sedimentology, **52**(6), 1207–1227. doi: 10.1111/j.1365-3091.2005.00736.x

Ćosović, V., Drobne, K., & Moro, A. (2004). Paleoenvironmental model for Eocene foraminiferal limestones of the Adriatic carbonate platform (Istrian Peninsula). Facies, **50**(1), 61–75. doi: 10.1007/s10347-004-0006-9

Davydov, V.I., & Arefifard, S. (2007). Permian fusulinid fauna of Peri-Gondwanan affinity from the Kalmard region, East-Central Iran and its significance for tectonics and paleogeography. Palaeontologia Electronica, **10**(2), 1–40.

Dunham, R.J. (1962). Classification of carbonate rocks according to depositional textures. In: Ham, W.E. (ed.), Classification of Carbonate Rocks: A Symposium Arranged by the Research Committee of the American Association of Petroleum Geologists, Tulsa, 1, 108–121.

Eftekharnezhad, J. (1980). Tectonic divisions of different parts of Iran regarding sedimentary basins. Journal of Oil Society, **82**, 19–28.

Embry, A.F., III, & Klovan, J.E. (1972). Absolute water depth limits of Late Devonian paleoecological zones. Geologische Rundschau, **61**(2), 672–686. doi: 10.1007/BF01896340

Emraninasab, B.H., Adabi, M.H., Majidifard, M.R., & Gadimvand, N.K. (2016). Facies interpretation, depositional environment and sequence stratigraphy of the Sartakht Formation in the Bakhshi, located in Kalmard Block, East-Central Iran. Open Journal of Geology, **06**(05), 314–329. doi: 10.4236/ojg.2016.65027

Emraninasab, B.H., Adabi, M.H., Majidifard, M.R., Gadimvand, N.K., & Erfani, S. (2017). Facies analysis and depositional environment of Upper Permian rocks in Darin section, East-Central Iran. Open Journal of Geology, **07**(03), 242–256. doi: 10.4236/ojg.2017.73017

Ernst, A., & Gorgij, M.N. (2013). Lower Permian bryozoan faunas from Kalmard area, central Iran. Neues Jahrbuch für Geologie und Paläontologie. Abhandlungen, **268**(3), 275–324. doi: 10.1127/0077-7749/2013/0330

Fa, X., Penghui, Z., Jinliang, Z., Jinshui, L., Guowei, H., Ming, Z., … Ningning, M. (2015). Diagenesis and diagenetic evolution of deltaic and neritic gas-bearing sandstones in the lower Mingyuefeng Formation of Paleogene, Lishui Sag, East China Sea Shelf Basin: Implications for depositional environments and sequence stratigraphy controls. [English edition]. Acta Geologica Sinica, **89**(5), 1625–1635. doi: 10.1111/1755-6724.12569

Fielding, C.R., Frank, T.D., & Isbell, J.L. (2008). Geological Society of America, Special Papers: **Vol. 441**. The late Paleozoic ice age – A review of current understanding and synthesis of global climate patterns (pp. 343–354). doi: 10.1130/2008.2441(24)

Flügel, E. (2010). Microfacies of Carbonate rocks. Berlin: Springer. doi: 10.1007/978-3-642-03796-2

Fournier, F., Montaggioni, L., & Borgomano, J. (2004). Paleoenvironments and high-frequency cyclicity from Cenozoic South-East Asian shallow-water carbonates:

A case study from the Oligo-Miocene buildups of Malampaya (Offshore Palawan, Philippines). Marine and Petroleum Geology, **21**(1), 1–21. doi: 10.1016/j.marpetgeo.2003.11.012

Fürsich, F.T., Wilmsen, M., Seyed-Emami, K., Schairer, G., & Majidifard, M.R. (2003). Platform-basin transect of a Middle to Late Jurassic large-scale carbonate platform system (Shotori Mountains, Tabas area, east-central Iran). Facies, **48**(1), 171–198. doi: 10.1007/BF02667538

Gregg, J.M. (1985). Regional epigenetic dolomitization in the Bonneterre Dolomite (Cambrian), southeastern Missouri. Geology, **13**(7), 503–506. doi: 10.1130/0091-7613(1985)13<503:REDITB>2.0.CO;2

Gregg, J.M., & Shelton, K.L. (1990). Dolomitization and dolomite neomorphism in the back reef facies of the Bonneterre and Davis formations (Cambrian), southeastern Missouri. Journal of Sedimentary Research, **60**, 495–562.

Gregg, J.M., & Sibley, D.F. (1984). Epigenetic dolomitization and the origin of xenotopic dolomite texture. Journal of Sedimentary Petrology, **54**, 908–931.

Haji Karim, K. (2006). Environment of Tanjero Formation as Inferred From Sedimentary Structures, Sulaimaniya area, Kurdistan Region, NE-Iraq. Kurdistan Academicians Journal, **4**(1), part 1.

Hallock, P., & Glenn, E.C. (1986). Larger foraminifera: A tool for paleoenvironmental analysis of Cenozoic carbonate depositional facies. Palaios, **1**(1), 55–64. doi: 10.2307/3514459

Hampson, G.J., & Storms, J.E. (2003). Geomorphological and sequence stratigraphic variability in wave-dominated, shoreface-shelf parasequences. Sedimentology, **50**(4), 667–701. doi: 10.1046/j.1365-3091.2003.00570.x

Hine, A.C. (1977). Lily Bank, Bahamas: History of an active oolite sand shoal. Journal of Sedimentary Research, **47**, 1544–1581.

Hopkins, J.C. (2004). Geometry and origin of dolomudstone reservoirs: Pekisko Formation (Lower Carboniferous), western Canada. Geological Society of London, Special Publications, **235**(1), 349–366. doi: 10.1144/GSL.SP.2004.235.01.15

Leckie, D.A., & Walker, R.G. (1982). Storm-and tide-dominated shorelines in Cretaceous Moosebar-Lower Gates interval-outcrop equivalents of Deep Basin gas trap in western Canada. AAPG Bulletin, **66**(2), 138–157.

Li, F., Qu, X., Du, L., Dai, T., Yang, J, Li, J., & Yang, C. (2016). Genetic processes and environmental significance of Lower Devonian brachiopod shell concentrations in Longmenshan area, Sichuan, China. Journal of Asian Earth Sciences, **115**, 393–403. doi: 10.1016/j.jseaes.2015.10.021

Lokier, S.W., Wilson, M.E., & Burton, L.M. (2009). Marine biota response to clastic sediment influx: A quantitative approach. Palaeogeography, Palaeoclimatology, Palaeoecology, **281**(1–2), 25–42. doi: 10.1016/j.palaeo.2009.07.007

MacEachern, J., Bann, K., Hampson, G., Steel, R., Burgess, P. & Dalrymple, R. (2008). The role of ichnology in refining shallow marine facies models. In: G.J. Hampson (ed.), Recent advances in models of siliciclastic shallow-marine stratigraphy. SEPM, Special Publications, 90, 73–116. doi: 10.2110/pec.08.90.0073

MacEachern, J.A., & Pemberton, S.G. (1992). Ichnological aspects of Cretaceous shoreface successions and shoreface variability in the Western Interior Seaway of North America. In S.G. Pemberton (Ed.), Applications of Ichnology to Petroleum Exploration. SEPM, Core Workshop Notes, 17, 57–84. doi: 10.2110/cor.92.01.0057

MacEachern, J.A., Pemberton, S.G., Gingras, M.K., & Bann, K.L. (2007). The ichnofacies paradigm: a fifty-year retrospective. In Trace Fossils (pp. 52–77). Amsterdam: Elsevier. doi: 10.1016/B978-044452949-7/50130-3

MacEachern, J.A., Stelck, C.R., & Pemberton, S.G. (1999a). Marine and marginal marine mudstone deposition: paleoenvironmental interpretations based on the integration of ichnology, palynology and foraminiferal paleoecology. In K.M. Bergman & J.W. Snedden (eds.), Isolated Shallow Marine Sand Bodies: Sequence Stratigraphic and Sedimentologic Interpretation. SEPM, Special Publications, 64, 205–225. doi: 10.2110/pec.99.64.0205

MacEachern, J.A., Zaitlin, B.A., & Pemberton, S.G. (1999b). A sharp-based sandstone of the Viking Formation, Joffre Field, Alberta, Canada: Criteria for recognition of transgressively incised shoreface complexes. Journal of Sedimentary Research, **69**(4), 876–892. doi: 10.2110/jsr.69.876

Mack, G.H., & James, W. (1985). Cyclic sedimentation in the mixed siliciclastic-carbonate Abo-Hueco transitional zone (Lower Permian), southwestern New Mexico. Sedimentary Research, **56**, 635–647.

Martini, R., Cirilli, S., Saurer, C., Abate, B., Ferruzza, G., & Cicero, G.L. (2007). Depositional environment and biofacies characterisation of the Triassic (Carnian to Rhaetian) carbonate succession of Punta Bassano (Marettimo Island, Sicily). Facies, **53**(3), 389–400. doi: 10.1007/s10347-007-0115-3

Metcalfe, I. (2002). Permian tectonic framework and palaeogeography of SE Asia. Journal of Asian Earth Sciences, **20**(6), 551–566. doi: 10.1016/S1367-9120(02)00022-6

Metcalfe, I. (2009). Late Palaeozoic and Mesozoic tectonic and palaeogeographical evolution of SE Asia. Geological Society of London, Special Publications, **315**(1), 7–23. doi: 10.1144/SP315.2

Muttoni, G., Gaetani, M., Kent, D.V., Sciunnach, D., Angiolini, L., Berra, F., & Zanchi, A. (2009a). The drift history of Iran from the Ordovician to the Triassic. Geological Society of London, Special Publications, **312**(1), 7–29. doi: 10.1144/SP312.2

Muttoni, G., Mattei, M., Balini, M., Zanchi, A., Gaetani, M., & Berra, F. (2009b). Opening of the Neo-Tethys Ocean and the Pangea B to Pangea A transformation during the Permian. GeoArabia, **14**(4), 17–48.

Myrow, P.M., & Southard, J.B. (1996). Tempestite deposition. Journal of Sedimentary Research, **66**, 875–887.

Myrow, P.M., Fischer, W., & Goodge, J.W. (2002). Wave-modified turbidites: Combined-flow shoreline and shelf deposits, Cambrian, Antarctica. Journal of Sedimentary Research, **72**(5), 641–656. doi: 10.1306/022102720641

Myrow, P.M., Tice, L., Archuleta, B., Clark, B., Taylor, J.F., & Ripperdan, R.L. (2004). Flat-pebble conglomerate: Its multiple origins and relationship to metre-scale depositional cycles. Sedimentology, **51**(5), 973–996. doi: 10.1111/j.1365-3091.2004.00657.x

Nichols, G. (2000). Sedimentology and Stratigraphy. Oxford: Blackwell.

Novak, V., Santodomingo, N., Rösler, A., Di Martino, E., Braga, J.C., Taylor, P.D., … Renema, W. (2013). Environmental reconstruction of a late Burdigalian (Miocene) patch reef in deltaic deposits (East Kalimantan, Indonesia). Palaeogeography, Palaeoclimatology, Palaeoecology, **374**, 110–122. doi: 10.1016/j.palaeo.2013.01.009

Nowrouzi, Z., Mahboubi, A., Moussavi-Harami, R., Mahmudy Gharaie, M.H., & Ghaemi, F. (2015). Facies analysis and sequence stratigraphy of Silurian carbonate ramps in the Turan (Kopeh-Dagh) and central Iran Plates with emphasis on Gondwana tectonic event. [English edition]. Acta Geologica Sinica, **89**(4), 1276–1295. doi: 10.1111/1755-6724.12528

Palma, R.M., López-Gómez, J., & Piethé, R.D. (2007). Oxfordian ramp system (La Manga Formation) in the Bardas Blancas area (Mendoza Province) Neuquén Basin, Argentina: Facies and depositional sequences. Sedimentary Geology, **195**(3–4), 113–134. doi: 10.1016/j.sedgeo.2006.07.001

Pemberton, S.G., MacEachern, J.A., & Brett, C. (1997). The ichnological signature of storm deposits: the use of trace fossils in event stratigraphy. In Paleontological Events: Stratigraphic, Ecological, and Evolutionary Implications (pp. 73–109). New York: Columbia University Press.

Pettijohn, F., Potter, P., & Siever, R. (1987). Sand and Sandstone (2nd ed.). New York: Springer. doi: 10.1007/978-1-4612-1066-5

Pomar, L. (2001a). Ecological control of sedimentary accommodation: Evolution from a carbonate ramp to rimmed shelf, Upper Miocene, Balearic Islands. Palaeogeography, Palaeoclimatology, Palaeoecology, **175**(1–4), 249–272. doi: 10.1016/S0031-0182(01)00375-3

Pomar, L. (2001b). Types of carbonate platforms: A genetic approach. Basin Research, **13**(3), 313–334. doi: 10.1046/j.0950-091x.2001.00152.x

Read, J.F. (1985). Carbonate platform facies models. AAPG Bulletin, **69**(1), 1–21.

Romero, J., Caus, E., & Rosell, J. (2002). A model for the palaeoenvironmental distribution of larger foraminifera based on late Middle Eocene deposits on the margin of the South Pyrenean basin (NE Spain). Palaeogeography, Palaeoclimatology, Palaeoecology, **179**(1–2), 43–56. doi: 10.1016/S0031-0182(01)00406-0

Ruban, D.A., Al-Husseini, M.I., & Iwasaki, Y. (2007). Review of Middle East Paleozoic plate tectonics. Geoarabia-Manama, **12**(3), 35–56.

Sardar Abadi, M., Kulagina, E.I., Voeten, D.F.A.E., Boulvain, F., & Da Silva, A.C. (2017). Sedimentologic and paleoclimatic reconstructions of carbonate factory evolution in the Alborz Basin (northern Iran) indicate a global response to Early Carboniferous (Tournaisian) glaciations. Sedimentary Geology, **348**, 19–36. doi: 10.1016/j.sedgeo.2016.11.011

Seidler, L., & Steel, R. (2001). Pinch-out style and position of tidally influenced strata in a regressive-transgressive wave-dominated deltaic sandbody, Twentymile Sandstone, Mesaverde Group, NW Colorado. Sedimentology, **48**(2), 399–414. doi: 10.1046/j.1365-3091.2001.00370.x

Shi, G., & Waterhouse, J. (2010). Late Palaeozoic global changes affecting high-latitude environments and biotas: An introduction. Palaeogeography, Palaeoclimatology, Palaeoecology, **298**(1–2), 1–16. doi: 10.1016/j.palaeo.2010.07.021

Shiekholslami, M.R., & Zamani, M. (1999). Geological map of the Halvan sheet (1:100000). Theran. Geological Survey of Iran.

Shinn, E.A. (1983). Tidal flat environment. In P.A. Scholl, D.G. Bebout, & C.H. Moore (eds.), Carbonate Depositional Environment. AAPG Memoirs, 33, 173–210.

Srivastava, V., & Singh, B. (2017). Facies analysis and depositional environments of the early Eocene Naredi Formation (Nareda locality), Kutch, Western India. Carbonates and Evaporites, **32**(3), 279–293. doi: 10.1007/s13146-016-0293-6

Stampfli, G.M. (1978). Étude géologique génerale de l'Elbourz oriental au sud de Gonbad-e-Qabus, Iran NE. Thèse Université de Génève, 329 pp.

Stocklin, J. (1968). Structural history and tectonics of Iran: A review. AAPG Bulletin, **52**(7), 1229–1258.

Testa, V., & Bosence, D.W. (1998). Carbonate-siliciclastic sedimentation on a high-energy, ocean-facing, tropical ramp, NE Brazil. Geological Society of London, Special Publications, **149**(1), 55–71. doi: 10.1144/GSL.SP.1999.149.01.05

Tucker, M.E., & Wright, V.P. (1990). Carbonate sedimentology. London: Blackwell. doi: 10.1002/9781444314175

Van Steenwinkel, M. (1990). Sequence stratigraphy from "spot" outcrops – example from a carbonate-dominated setting: Devonian-Carboniferous transition, Dinant synclinorium (Belgium). Sedimentary Geology, **69**(3–4), 259–280. doi: 10.1016/0037-0738(90)90053-V

Vaziri-Moghaddam, H., Seyrafian, A., Taheri, A., & Motiei, H. (2010). Oligocene-Miocene ramp system (Asmari Formation) in the NW of the Zagros Basin, Iran: Microfacies, paleoenvironment and depositional sequence. Revista Mexicana de Ciencias Geológicas, **27**(1), 56–71.

Wilmsen, M., Fürsich, F.T., Seyed-Emami, K., Majidifard, M.R., & Zamani-Pedram, M. (2010). Facies analysis of a large-scale Jurassic shelf-lagoon: The Kamar-e-Mehdi Formation of east-central Iran. Facies, **56**(1), 59–87. doi: 10.1007/s10347-009-0190-8

Wilson, J.L. (1975). Carbonate facies in geologic history. New York: Springer. doi: 10.1007/978-1-4612-6383-8

Zanchi, A., Zanchetta, S., Berra, F., Mattei, M., Garzanti, E., Molyneux, S., … Sabouri, J. (2009). The Eo-Cimmerian (Late? Triassic) orogeny in north Iran. Geological Society of London, Special Publications, **312**(1), 31–55. doi: 10.1144/SP312.3

Zhang, Y., Shi, G., & Shen, S.Z. (2013). A review of Permian stratigraphy, palaeobiogeography and palaeogeography of the Qinghai-Tibet Plateau. Gondwana Research, **24**(1), 55–76. doi: 10.1016/j.gr.2012.06.010

Manuscript received: September 28th, 2018.
Revised version accepted by the Stuttgart editor: January 07th, 2019.

Addresses of the authors:

Samira Taghdisi Nikbakht, Payman Rezaee (corresponding author), Department of Geology, Faculty of Sciences, University of Hormozgan, Iran;
e-mail: p.rezaee@hormozgan.ac.ir

Reza Moussavi-Harami, Mohammad Khanehbad, Farzin Ghaemi, Department of Geology, Faculty of Sciences, Ferdowsi University of Mashhad, Iran.